International Journal of Bifurcation and Chaos, Vol. 26, No. 14 (2016) 1630040 (24 pages)

DOI: 10.1142/S0218127416300408

Dangerous Bifurcations Revisited

Viktor Avrutin
IST, University of Stuttgart, Germany
avrutin.viktor@gmail.com

Zhanybai T. Zhusubaliyev
Southwest State University, Kursk, Russia
zhanybai@hotmail.com

Arindam Saha* and Soumitro Banerjee†
Department of Physical Sciences,
Indian Institute of Science Education and Research Kolkata,
Mohanpur Campus, Nadia-741246, West Bengal, India
**arindamsaha1507@gmail.com*
†*soumitro@iiserkol.ac.in*

Irina Sushko
Institute of Mathematics,
National Academy of Sciences of Ukraine, Ukraine
sushko@imath.kiev.ua

Laura Gardini
Department of Economics, Society, Politics,
University of Urbino, Italy
laura.gardini@uniurb.it

Received August 31, 2016

A dangerous border collision bifurcation has been defined as the dynamical instability that occurs when the basins of attraction of stable fixed points shrink to a set of zero measure as the parameter approaches the bifurcation value from either side. This results in almost all trajectories diverging off to infinity at the bifurcation point, despite the eigenvalues of the fixed points before and after the bifurcation being within the unit circle. In this paper, we show that similar bifurcation phenomena also occur when the stable orbit in question is of a higher periodicity or is chaotic. Accordingly, we propose a generalized definition of dangerous bifurcation suitable for any kind of attracting sets. We report two types of dangerous border collision bifurcations and show that, in addition to the originally reported mechanism typically involving singleton saddle cycles, there exists one more situation where the basin boundary is formed by a repelling closed invariant curve.

Keywords: Dangerous bifurcation; border collision bifurcation; piecewise smooth maps; border collision normal form.

1. Introduction

One of the main features of piecewise smooth systems is their ability to demonstrate border collision bifurcations which occur when a fixed point or a periodic orbit collides with a switching manifold in the state space. This results in a very rich array of bifurcation phenomena which include a direct transition from a periodic behavior to chaos [Nusse & Yorke, 1992, 1995; Banerjee & Grebogi, 1999; Di Bernardo *et al.*, 1999] or quasiperiodicity [Zhusubaliyev *et al.*, 2006], robust chaos [Banerjee *et al.*, 1998], coexistence of many (even an infinite number of) attractors [Dutta *et al.*, 1999; Simpson, 2014], etc. Examples of systems which may be described by piecewise smooth maps can be found in such areas as electronics (circuits including any kind of switches) [Deane & Hamill, 1990; Kousaka *et al.*, 1999; Banerjee *et al.*, 2000; Banerjee & Verghese, 2001; Zhusubaliyev & Mosekilde, 2003] and mechanics (systems with impacts and/or dry friction) [Nordmark, 1991; Armstrong-Hélouvry *et al.*, 1994; Brogliato, 1999; Leine & Nijmeijer, 2013], as well as in economics and social sciences [Puu & Sushko, 2002, 2006; Bischi & Merlone, 2010; Matsuyama *et al.*, 2016].

In this paper, we focus on the specific bifurcation phenomenon known as "dangerous border collision bifurcation". In the past, the term "dangerous" has been used as adjective to many different kinds of dynamical phenomena; even a saddle-node bifurcation or a subcritical period-doubling bifurcation has been sometimes considered as "dangerous." But in the context of piecewise smooth systems the term "dangerous border collision bifurcation" has a specific meaning.

Hassouneh *et al.* [2004] first reported a situation where the fixed point of a system remains stable before and after a bifurcation, and yet at the bifurcation point the orbits diverge from almost all initial conditions, because the basin of attraction of the fixed point shrinks to a set of measure zero. They termed it dangerous border collision bifurcation because the eigenvalues of the system do not give any signal of the impending catastrophe. The prediction of this type of instability, being in no way related to eigenvalues, requires one to analyze the global structure of the phase space.

In [Hassouneh *et al.*, 2004] the authors reported the occurrence of dangerous border collision bifurcation in the 2D border collision form map (given in Sec. 2) and obtained numerically some of the parameter space regions where this phenomenon was observed to occur. The mechanism behind the occurrence of dangerous border collision bifurcation was explained in [Ganguli & Banerjee, 2005]. The authors analytically obtained the parameter space regions, which were the same as those obtained numerically in [Hassouneh *et al.*, 2004]. Even though the Jacobian of the fixed point is not really defined at the bifurcation point, Do *et al.* [Do, 2007; Do & Baek, 2006] showed that the fixed point has the character of a saddle.

In this line of work the dangerous border collision bifurcation referred to the situation where attractors before and after the bifurcation are fixed points. Our subsequent work [Gardini *et al.*, 2009] has revealed that similar situation may also arise when some other stable orbit (not necessarily a fixed point) occurs before and after the bifurcation. This has necessitated a broadening of the definition of dangerous border collision bifurcation.

The paper is organized as follows. In Sec. 2 the original definition of a dangerous bifurcation is recalled. Based on that, in Sec. 3 we provide an extended definition and then in Sec. 4 we illustrate it by several examples of bifurcations occurring in the 2D border collision normal form. Thereafter, in Sec. 5 we discuss two types of dangerous bifurcation. The first one (Sec. 5.1) is related to the case where the boundary of the basin associated with divergent trajectories is unbounded (extends to infinity). In particular, the case in which this boundary is formed by the stable manifold of a singleton saddle cycle as discussed for example in [Ganguli & Banerjee, 2005] in the context of the original definition of a dangerous border collision bifurcation belongs to this type. The second type (Sec. 5.2), related to the case where the boundary of the basin associated with divergent trajectories is bounded and formed by a closed invariant curve, has not been reported before.

2. Original Definition of a Dangerous Border Collision Bifurcation

Originally, in [Hassouneh *et al.*, 2004], a dangerous bifurcation was defined as a subclass of border collision bifurcations with the following distinguishing property:

> In this bifurcation, although an attracting fixed point exists for all parameter values

before and after the critical bifurcation parameter value, a striking feature occurs in which the bifurcation typically leads to "unbounded behavior" of orbits as a system parameter is slowly varied through its bifurcation value in each of the two directions. At the bifurcation value, for the corresponding piecewise smooth linear map of the piecewise smooth system, all orbits with nonzero initial condition diverge to infinity.[1]

The occurrence of a dangerous bifurcation in the sense of this definition in the continuous piecewise-linear 2D border collision normal form[2]

$$X_{n+1} = F(X_n, \mu) = \begin{cases} A_{\mathcal{L}} X_n + B & \text{if } x_n \le 0 \\ A_{\mathcal{R}} X_n + B & \text{if } x_n > 0 \end{cases} \tag{1a}$$

with

$$X_n = \begin{pmatrix} x_n \\ y_n \end{pmatrix}, \quad A_{\mathcal{L}/\mathcal{R}} = \begin{pmatrix} \tau_{\mathcal{L}/\mathcal{R}} & 1 \\ -\delta_{\mathcal{L}/\mathcal{R}} & 0 \end{pmatrix}, \quad B = \mu \begin{pmatrix} 1 \\ 0 \end{pmatrix} \tag{1b}$$

is illustrated in Fig. 1. In this figure, stable fixed points and their basins of attraction are shown before the bifurcation (for $\mu < 0$) and after the bifurcation (for $\mu > 0$). The trajectories that started outside these basins diverge. As μ tends to zero from either side, the basins of attraction of both fixed points shrink to a set of zero measure. Accordingly, at $\mu = 0$ orbits starting at typical initial conditions diverge. Since the piecewise-linear normal form map embodies the local dynamics of a generic piecewise smooth map in the neighborhood of the borderline (under some nondegeneracity conditions), a diverging orbit in the normal form map signifies a locally divergent behavior in the context of the piecewise smooth system. Therefore, a dangerous bifurcation in a generic piecewise smooth system is manifested in an abrupt onset of a different dynamics as parameters approach the bifurcation value from either side.

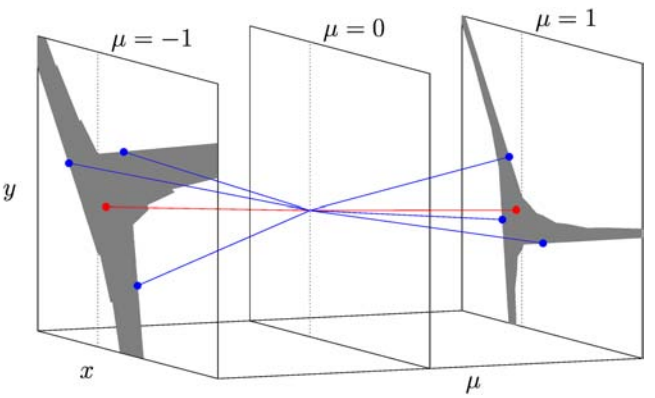

Fig. 1. Dangerous transition from one stable fixed point for $\mu < 0$ to another one for $\mu > 0$. The basins of attraction (shown in gray) shrink to zero as μ approaches zero from either side, so that at $\mu = 0$ orbits starting at typical initial values diverge. The complementary set related to divergence is shown in white.

In the following, when referring to cycles of the normal form (1) we use the standard symbolic coding and associate with a period-m cycle $\{p_0, p_1, \ldots, p_{m-1}\}$ a symbolic sequence $\sigma = \sigma_0\sigma_1\cdots\sigma_{m-1}$ with $\sigma_j = \mathcal{L}$ if the point $p_j = (x_j, y_j)^{\mathrm{T}}$ is located in the left half-plane, i.e. if $x_j < 0$ and $\sigma_j = \mathcal{R}$ if $x_j > 0$, $j = 0, \ldots, m-1$.[3] The cycle itself is denoted by $\mathcal{O}_\sigma$, its existence region in the parameter space by $\mathcal{P}_\sigma$. The subregions of $\mathcal{P}_\sigma$ in which $\mathcal{O}_\sigma$ is stable/unstable are denoted by $\mathcal{P}^s_\sigma$ and $\mathcal{P}^u_\sigma$, respectively. Where it is necessary, we specify by an upper index also if a particular result applies for $\mu > 0$ or for $\mu < 0$. For example $\mathcal{P}^{(+)}_\sigma \subset \mathcal{P}_\sigma$ refers to the part of $\mathcal{P}_\sigma$ located above the boundary $\mu = 0$ (i.e. for $\mu > 0$), and $\mathcal{P}^{(-)}_\sigma \subset \mathcal{P}_\sigma$ refers to the part located below (for $\mu < 0$). The basin of attraction of $\mathcal{O}_\sigma$ is denoted by $\mathcal{B}(\mathcal{O}_\sigma)$. In addition, the divergent domain, i.e. the set of initial values leading to divergent trajectories, is denoted by $\mathcal{B}_{\mathrm{div}}$.

For the bifurcations that a cycle $\mathcal{O}_\sigma$ may undergo, the following notation is used. First, the cycle may appear/disappear via a *border collision fold* bifurcation at which also a complementary cycle $\mathcal{O}_\varrho$ appears/disappears and the set of parameters at which this occurs is denoted by $\xi_{\sigma/\varrho}$.[4]

[1]Strictly speaking, it should say *almost all* orbits with nonzero initial condition diverge to infinity.

[2]Originally introduced in [Nusse & Yorke, 1992], this normal form has four parameters $\tau_{\mathcal{L}}$, $\tau_{\mathcal{R}}$, $\delta_{\mathcal{L}}$, $\delta_{\mathcal{R}}$ ($\tau_{\mathcal{L}/\mathcal{R}}$, $\delta_{\mathcal{L}/\mathcal{R}}$ for short) corresponding to the trace and determinant of the Jacobians evaluated at fixed points on the left and right sides of the border, and the parameter μ which controls the border collision.

[3]For the purposes of the present paper we do not need to specify symbolic sequence of cycles containing points on the boundary, i.e. points with $x_j = 0$.

[4]Recall that cycles $\mathcal{O}_\sigma$ and $\mathcal{O}_\varrho$ are called complementary if the symbolic sequences σ and ϱ differ by one letter. Accordingly, an m-cycle $\mathcal{O}_\sigma$ may be involved in m different border collision fold bifurcations.

The cycle may also appear/disappear via a *degenerate transcritical* bifurcation, say η_σ, at which the points of the cycle approach infinity, while one eigenvalue tends to $+1$ [Sushko & Gardini, 2010; Avrutin *et al.*, 2010]. These two bifurcation boundaries may confine the region $\mathcal{P}_\sigma$. Inside this region, the cycle may change its stability via a *degenerate flip bifurcation* θ_σ occurring when an eigenvalue of the cycle crosses -1 [Sushko & Gardini, 2010].

The appearance of dangerous bifurcations in map (1) under variation of the parameter μ can be explained by observing that, as long as we do not change the sign of μ, changing the absolute value of μ leads only to a linear scaling of the complete phase space. As

$$F(X, \alpha\mu) = \alpha F\left(\frac{X}{\alpha}, \mu\right) \quad \forall\, X \in \mathbb{R}^2,\ \ \forall\, \alpha > 0 \tag{2}$$

each bounded invariant set of map (1) scales linearly with μ, and in particular shrinks to zero as μ tends to zero. Therefore, for map (1) the necessary and sufficient condition for a dangerous border collision bifurcation according to the definition given above is the *coexistence of stable* (*but not globally attracting*) *fixed points and diverging trajectories before and after the bifurcation.*

It is well known that fixed points $\mathcal{O}_\mathcal{L}$ and $\mathcal{O}_\mathcal{R}$ of map (1) are stable (for $\mu < 0$ and $\mu > 0$, respectively) in the parameter space region

$$\mathcal{P} = \{\delta_{\mathcal{L}/\mathcal{R}}, \tau_{\mathcal{L}/\mathcal{R}}; |\tau_{\mathcal{L}/\mathcal{R}}| < 1 + \delta_{\mathcal{L}/\mathcal{R}}, |\delta_{\mathcal{L}/\mathcal{R}}| < 1\}. \tag{3}$$

Hence, dangerous bifurcations in the sense of the original definition can occur in map (1) only if the conditions (3) are satisfied.

Figure 2 shows that the boundary of the basin of attraction of the fixed point

$$\mathcal{O}_\mathcal{L} = \frac{\mu}{1 - \tau_\mathcal{L} + \delta_\mathcal{L}}(1, -\delta_\mathcal{L})^{\mathrm{T}} \tag{4}$$

before the bifurcation is constituted by the stable manifold of the period-3 saddle cycle $\mathcal{O}_{\mathcal{R}\mathcal{L}^2}$. After the bifurcation the basin boundary of the fixed point

$$\mathcal{O}_\mathcal{R} = \frac{\mu}{1 - \tau_\mathcal{R} + \delta_\mathcal{R}}(1, -\delta_\mathcal{R})^{\mathrm{T}} \tag{5}$$

is formed by the stable manifold of another period-3 saddle cycle $\mathcal{O}_{\mathcal{L}\mathcal{R}^2}$.

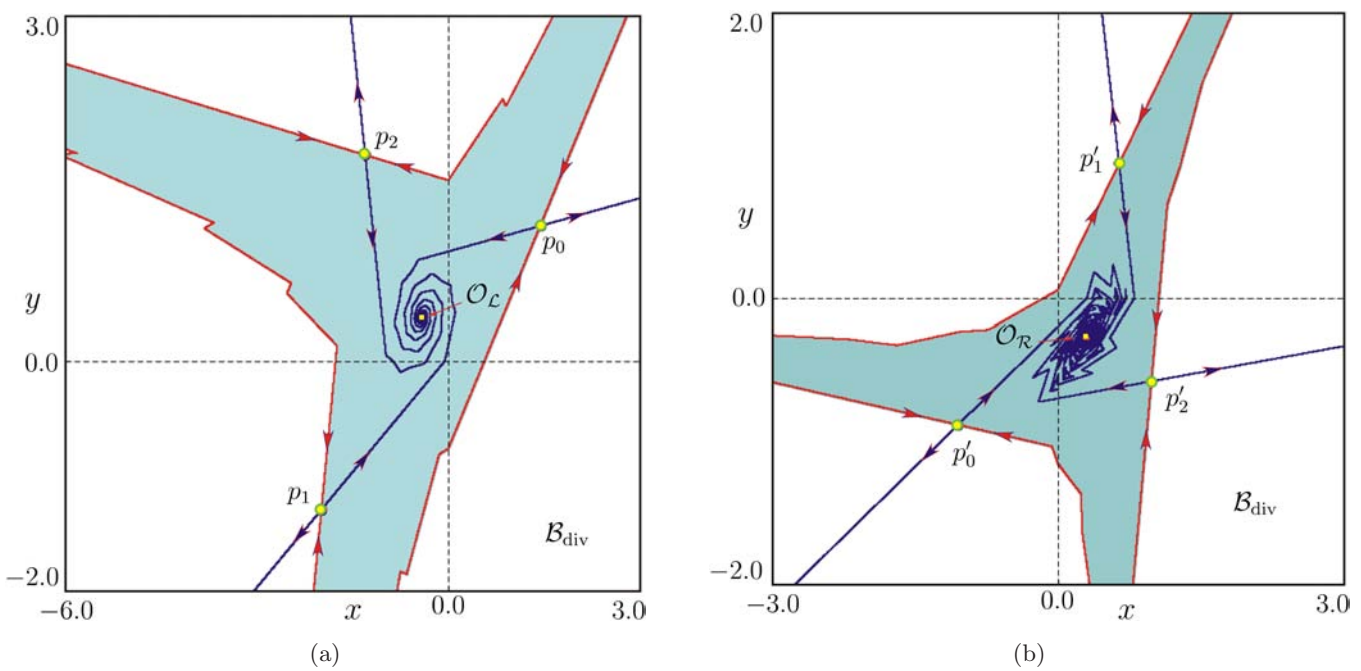

(a) (b)

Fig. 2. Structure of the state space (a) before and (b) after a dangerous border collision bifurcation leading from a stable fixed point $\mathcal{O}_\mathcal{L}$ to a stable fixed point $\mathcal{O}_\mathcal{R}$. The basins of attraction $\mathcal{B}(\mathcal{O}_\mathcal{L})$, $\mathcal{B}(\mathcal{O}_\mathcal{R})$ are shown in light blue. Before the bifurcation, the basin $\mathcal{B}(\mathcal{O}_\mathcal{L})$ is separated from the domain of diverging trajectories $\mathcal{B}_{\mathrm{div}}$ by the stable manifold of the 3-cycle $\mathcal{O}_{\mathcal{R}\mathcal{L}^2} = \{p_0, p_1, p_2\}$; after the bifurcation $\mathcal{B}(\mathcal{O}_\mathcal{R})$ is separated from $\mathcal{B}_{\mathrm{div}}$ by the stable manifold of the 3-cycle $\mathcal{O}_{\mathcal{L}\mathcal{R}^2} = \{p'_0, p'_1, p'_2\}$. Stable manifolds are shown in red, unstable in blue. Parameters: $\tau_\mathcal{L} = -0.5$, $\tau_\mathcal{R} = -1.5$, $\delta_\mathcal{L} = \delta_\mathcal{R} = 0.9$, (a) $\mu = -1$; (b) $\mu = 1$.

In [Ganguli & Banerjee, 2005] it is shown that these bifurcations can be explained considering for $\mu > 0$ the stable basic cycles $\mathcal{O}_{\mathcal{RL}^n}$ and their complementary unstable cycles $\mathcal{O}_{\mathcal{RL}^{n-1}\mathcal{R}}$, $n \geq 3$. It was shown that the regions of existence of such a pair of complementary cycles in the parameter space are different. The region of the existence of the stable cycle $\mathcal{P}_{\mathcal{RL}^n}$ is a subset of the region of the existence of the unstable cycle $\mathcal{P}_{\mathcal{RL}^{n-1}\mathcal{R}}$. If for some n the region $\mathcal{P}_{\mathcal{RL}^{n-1}\mathcal{R}} \backslash \mathcal{P}_{\mathcal{RL}^n}$ overlaps with the region $\mathcal{P}$ given by Eq. (3), then for $\mu > 0$ the stable fixed point exists and the stable manifold of the unstable cycle $\mathcal{P}_{\mathcal{RL}^{n-1}\mathcal{R}}$ belongs to the boundary $\partial\mathcal{B}_{\rm div}$. Since the complementary orbit $\mathcal{P}_{\mathcal{RL}^n}$ does not exist, if there are no attracting sets outside this basin of attraction, then all trajectories starting from there diverge.

For $\mu < 0$ the situation can be described similarly, by interchanging the letters $\mathcal{L}$ and $\mathcal{R}$. In this way, in [Ganguli & Banerjee, 2005] the regions leading to dangerous border collision bifurcations were determined by calculating the existence boundaries for the cycles $\mathcal{O}_{\mathcal{RL}^n}$ and $\mathcal{O}_{\mathcal{RL}^{n-1}\mathcal{R}}$.

3. Extended Definition of a Dangerous Border Collision Bifurcation

The question arises why the definition of dangerous bifurcation should be restricted to fixed points only. Indeed, if the attractor before the bifurcation is given by a fixed point and the attractor after the bifurcation by an n-cycle, $n \geq 2$, as shown in [Gardini *et al.*, 2009] and in the Example 1 below, then the main distinguishing feature of the bifurcation remains unchanged, i.e. at the bifurcation point an infinitely small deviation leads to divergence. Nowadays, many kinds of border collision bifurcations are known, that lead to the appearance of attractors of different kinds, and also to the appearance of many (even infinity many) coexisting attractors [Simpson, 2014]. There is no reason why these bifurcations cannot be dangerous. Therefore, it is natural to extend the original definition of a dangerous bifurcation in the following way:

A border collision bifurcation in a piecewise smooth system is called dangerous, when the related border collision normal form (1) for $\mu < 0$ and for $\mu > 0$ has

(i) at least one bounded attractor,

(ii) a set of initial conditions with a positive measure that leads to divergent behavior.

Note that the scaling property (2) together with (ii) imply that as the parameters approach the bifurcation value from either side, the basins of attraction of all attractors tend to zero measure sets and at the bifurcation point, all trajectories starting at typical initial values diverge.

Similar to the one proposed in [Gardini *et al.*, 2009], this definition extends the previous one, as it includes the cases in which not only fixed points but other attractors are involved.

Over the years many classes of border collision bifurcation have been introduced [Di Bernardo *et al.*, 1999; Banerjee & Grebogi, 1999]. Out of these, only the case of "persistence border collision bifurcation" was included in the original definition of dangerous bifurcation. In this extended definition, all the classes are shown to be capable of displaying dangerous border collision bifurcation under suitable parameter conditions.

4. Examples of Dangerous Bifurcations

Before discussing mechanisms which may lead to dangerous border collision bifurcations in the sense of the extended definition given above, let us first illustrate it by a few examples showing several cases which do not fit the original definition of dangerous border collision bifurcations but are covered by the extended one.

Example 1. *Fixed point ↔ n-cycle*

Probably the simplest example of a dangerous bifurcation which does not fit the original definition but fits the extended one is illustrated in Fig. 3. Here, the situation before the bifurcation is as in the previous example (the fixed point $\mathcal{O}_{\mathcal{L}}$ before the bifurcation is stable and its basin boundary is constituted by the stable manifold of the period-3 saddle cycle $\mathcal{O}_{\mathcal{RL}^2}$). But after the bifurcation, the fixed point $\mathcal{O}_{\mathcal{R}}$ of map (1) is unstable, and there is a stable 2-cycle $\mathcal{O}_{\mathcal{LR}}$. The boundary between the basin $\mathcal{B}(\mathcal{O}_{\mathcal{LR}})$ and the divergent domain $\mathcal{B}_{\rm div}$ is given by the stable manifold of the period-3 saddle cycle $\mathcal{O}_{\mathcal{LR}^2}$. As before, the orbits starting at initial values outside these basins diverge, and the basins shrink to zero as μ approaches zero from either side.

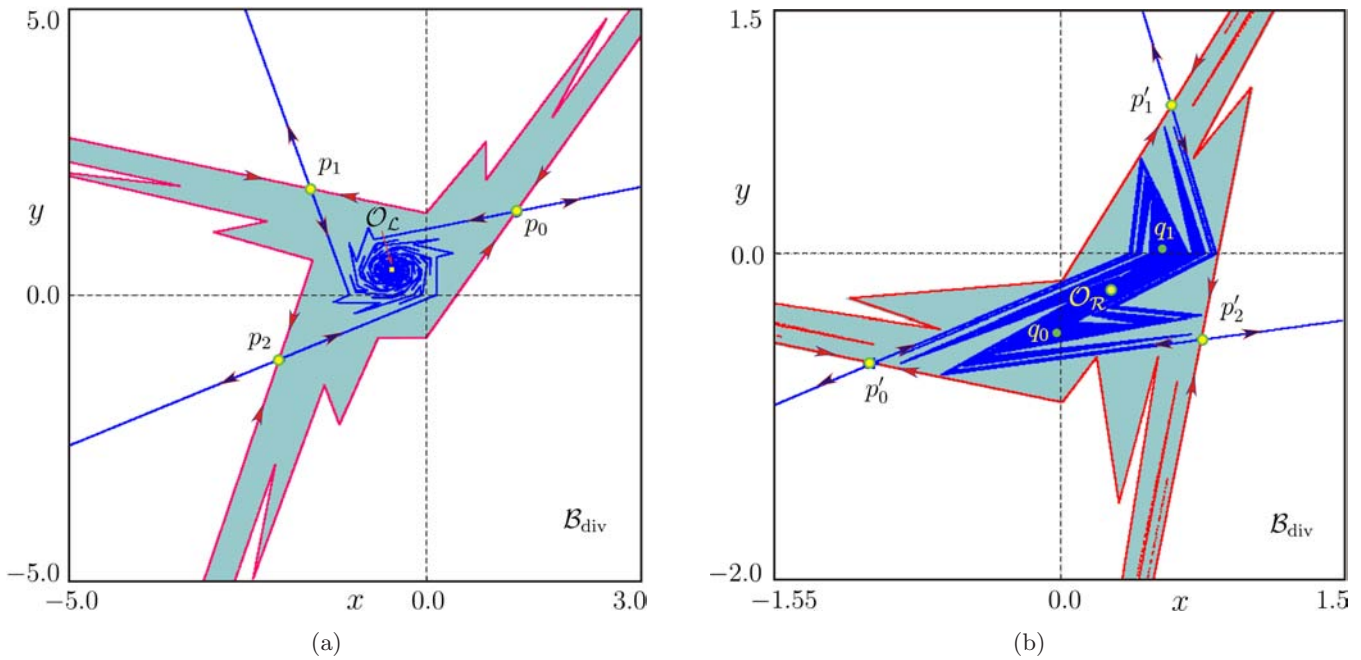

Fig. 3. Structure of the state space (a) before and (b) after a dangerous border collision bifurcation leading from a stable fixed point $\mathcal{O}_\mathcal{L}$ to a stable 2-cycle $\mathcal{O}_{\mathcal{LR}} = \{q_0, q_1\}$. The corresponding basins of attraction are shown in light blue. Before the bifurcation the basin $\mathcal{B}(\mathcal{O}_\mathcal{L})$ is separated from the divergent domain $\mathcal{B}_{\rm div}$ by the stable manifold of the 3-cycle $\mathcal{O}_{\mathcal{RL}^2} = \{p_0, p_1, p_2\}$, after the bifurcation the basin $\mathcal{B}(\mathcal{O}_{\mathcal{LR}})$ is separated from $\mathcal{B}_{\rm div}$ by the stable manifold of the 3-cycle $\mathcal{O}_{\mathcal{LR}^2} = \{p'_0, p'_1, p'_2\}$. Parameters: $\tau_\mathcal{L} = -0.25$, $\tau_\mathcal{R} = -2$, $\delta_\mathcal{L} = \delta_\mathcal{R} = 0.9$, (a) $\mu = -1$; (b) $\mu = 1$. The corresponding point in the parameter plane $(\tau_\mathcal{L}, \tau_\mathcal{R})$ is marked with A in Fig. 10.

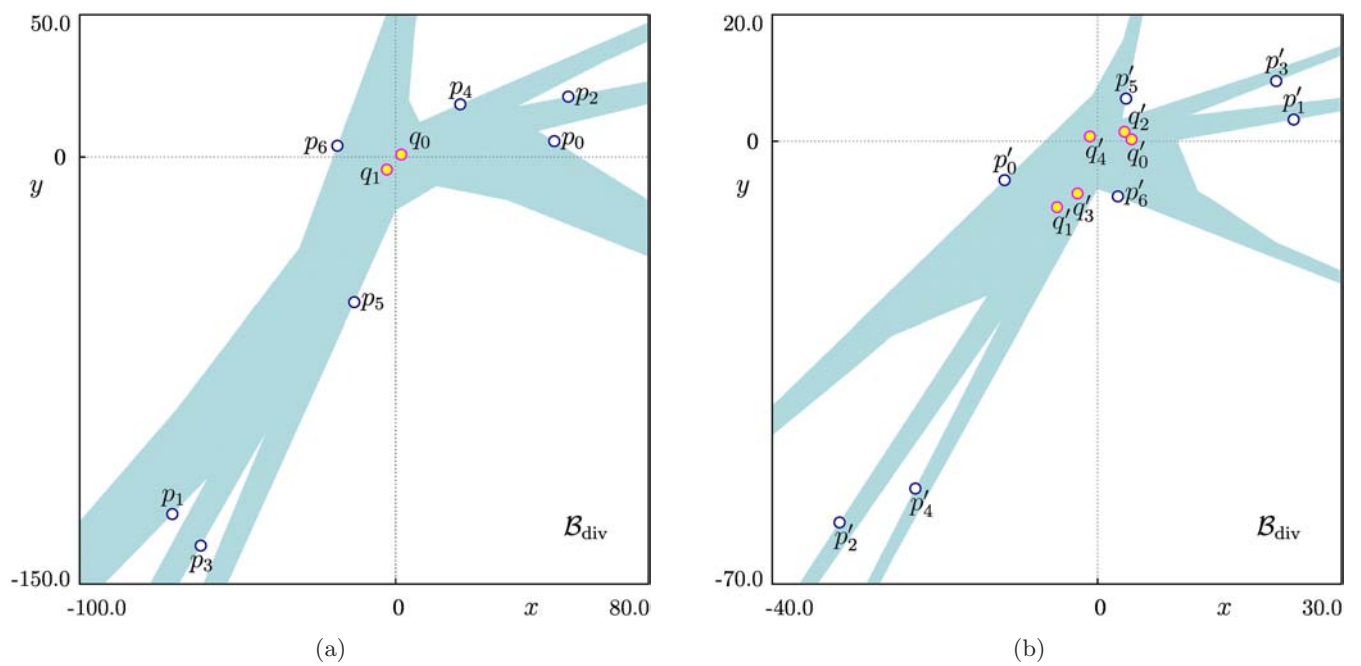

Fig. 4. Structure of the state space (a) before and (b) after a dangerous border collision bifurcation leading from a stable 2-cycle $\mathcal{O}_{\mathcal{RL}} = \{q_0, q_1\}$ to a stable 5-cycle $\mathcal{O}_{\mathcal{RLRL}^2} = \{q'_0, q'_1, \ldots, q'_4\}$. Before the bifurcation the basin $\mathcal{B}(\mathcal{O}_{\mathcal{LR}})$ is separated from the divergent domain $\mathcal{B}_{\rm div}$ by the stable manifold of the 7-cycle $\mathcal{O}_{(\mathcal{RL})^2\mathcal{RL}^2} = \{p_0, p_1, \ldots, p_6\}$; after the bifurcation the basin $\mathcal{B}(\mathcal{O}_{\mathcal{RLRL}^2})$ is separated from $\mathcal{B}_{\rm div}$ by the stable manifold of the 7-cycle $\mathcal{O}_{(\mathcal{LR})^2\mathcal{LR}^2} = \{p'_0, p'_1, \ldots, p'_6\}$. Parameters: $\tau_\mathcal{L} = -2.56$, $\tau_\mathcal{R} = -1.5$, $\delta_\mathcal{L} = 0.3$, $\delta_\mathcal{R} = 2.5$, (a) $\mu = -1$; (b) $\mu = 1$.

Example 2. *k-cycle ↔ m-cycle*

Since [Nusse & Yorke, 1992], it is known that a border collision bifurcation in map (1) may lead from one stable cycle with a period $k > 1$ to a different stable cycle with another period $m > 1$, $m \neq k$, not involving any stable fixed points. Such bifurcations may also be dangerous, as illustrated in Fig. 4. In the presented case, as μ is varied from negative to positive values, we observe a transition from a stable 2-cycle $\mathcal{O}_{\mathcal{RL}}$ to a stable 5-cycle $\mathcal{O}_{\mathcal{RLRL}^2}$. Before the bifurcation, the basin $\mathcal{B}(\mathcal{O}_{\mathcal{RL}})$ is separated from the divergent domain $\mathcal{B}_{\text{div}}$ by the stable manifold of the saddle 7-cycle $\mathcal{O}_{(\mathcal{RL})^2\mathcal{RL}^2}$. After the bifurcation, the basin $\mathcal{B}(\mathcal{O}_{\mathcal{RLRL}^2})$ is separated from $\mathcal{B}_{\text{div}}$ by the stable manifold of the saddle 7-cycle $\mathcal{O}_{(\mathcal{LR})^2\mathcal{LR}^2}$.

Example 3. *Multiple cycles ↔ multiple cycles*

Border collision bifurcations may lead to appearance (or disappearance) of multiple attractors [Dutta *et al.*, 1999; Sushko & Gardini, 2008; Avrutin *et al.*, 2012]. Such a bifurcation can also be dangerous, as illustrated in Fig. 5. In the presented case, before the bifurcation there are two attractors, namely the stable 2-cycle $\mathcal{O}_{\mathcal{LR}}$ and the stable 9-cycle $\mathcal{O}_{(\mathcal{RL})^4\mathcal{R}}$. Their basins are separated from the divergent domain $\mathcal{B}_{\text{div}}$ by the period-7 saddle cycle $\mathcal{O}_{(\mathcal{RL})^3\mathcal{L}}$. As a result of a dangerous multiple attractor bifurcation these two attractors disappear, and three new attractors appear: the stable fixed point $\mathcal{O}_{\mathcal{R}}$, the stable 5-cycle $\mathcal{O}_{\mathcal{RLRL}^2}$ and the stable 12-cycle $\mathcal{O}_{(\mathcal{LR})^3(\mathcal{RL})^3}$. Their basins are separated from the divergent domain by the stable manifold of a saddle 7-cycle $\mathcal{O}_{(\mathcal{RL})^3\mathcal{R}}$.

Example 4. *Fixed point ↔ chaotic attractor*

A transition from a fixed point directly to a chaotic attractor can occur in a border collision bifurcation. It is in fact quite common and occurs over large regions in the parameter space especially if the determinants $\delta_{\mathcal{L}}$, $\delta_{\mathcal{R}}$ are negative. Figure 6 shows that such a bifurcation can also be dangerous [Gardini *et al.*, 2009]. In the presented example, before

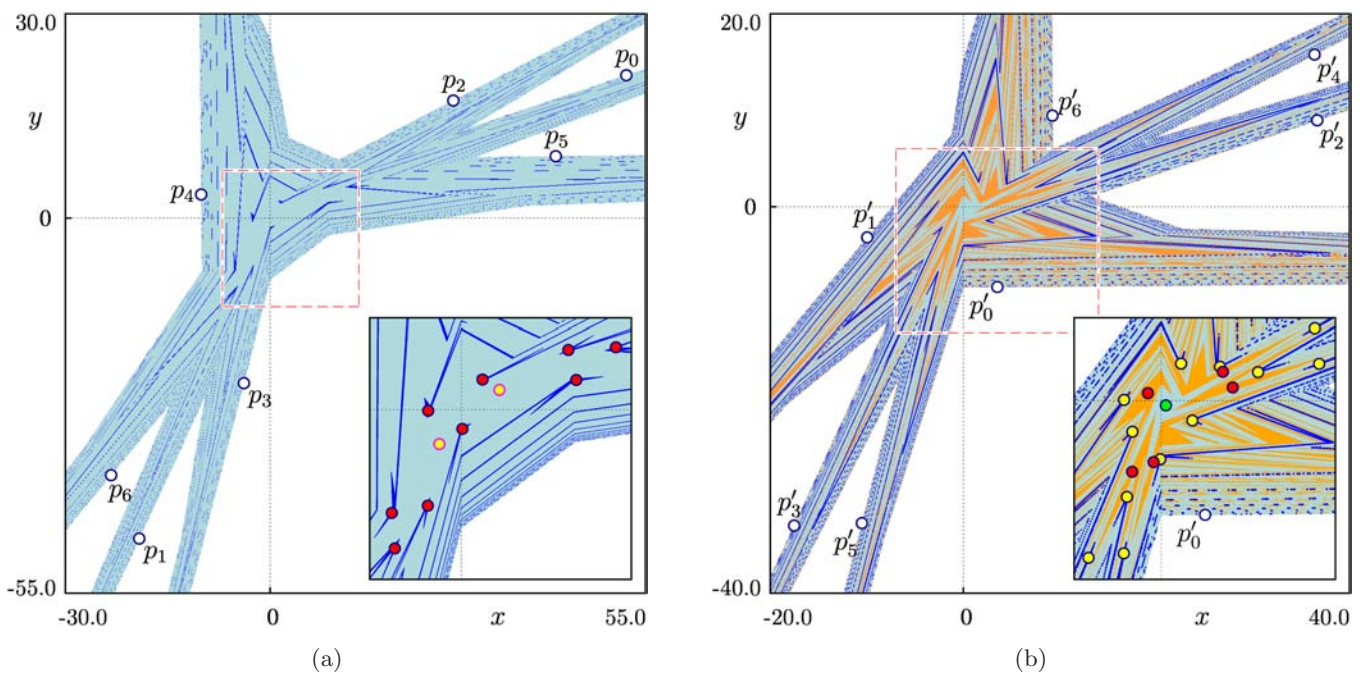

(a) (b)

Fig. 5. Structure of the state space (a) before and (b) after a dangerous border collision bifurcation leading from two coexisting attractors (2-cycle $\mathcal{O}_{\mathcal{LR}}$ and 9-cycle $\mathcal{O}_{(\mathcal{RL})^4\mathcal{R}}$, marked in the inset by yellow and red points, respectively) to three coexisting attractors (fixed point $\mathcal{O}_{\mathcal{R}}$, 5-cycle $\mathcal{O}_{\mathcal{RLRL}^2}$ and 12-cycle $\mathcal{O}_{(\mathcal{LR})^3(\mathcal{RL})^3}$, marked in the inset by green, red and yellow points, respectively). Before the bifurcation the boundary of the divergent domain $\mathcal{B}_{\text{div}}$ includes the stable set of the 7-cycle $\mathcal{O}_{(\mathcal{RL})^2\mathcal{LRL}} = \{p_0, p_1, \ldots, p_r\}$; after the bifurcation it includes the stable set of the 7-cycle $\mathcal{O}_{(\mathcal{RL})^3\mathcal{R}} = \{p'_0, p'_1, \ldots, p'_6\}$. Parameters: $\tau_{\mathcal{L}} = -3.9$, $\tau_{\mathcal{R}} = -0.75$, $\delta_{\mathcal{L}} = \delta_{\mathcal{R}} = 0.9$, (a) $\mu = -1$; (b) $\mu = 1$. The corresponding point in the parameter plane $(\tau_{\mathcal{L}}, \tau_{\mathcal{R}})$ is marked with B in Fig. 10.

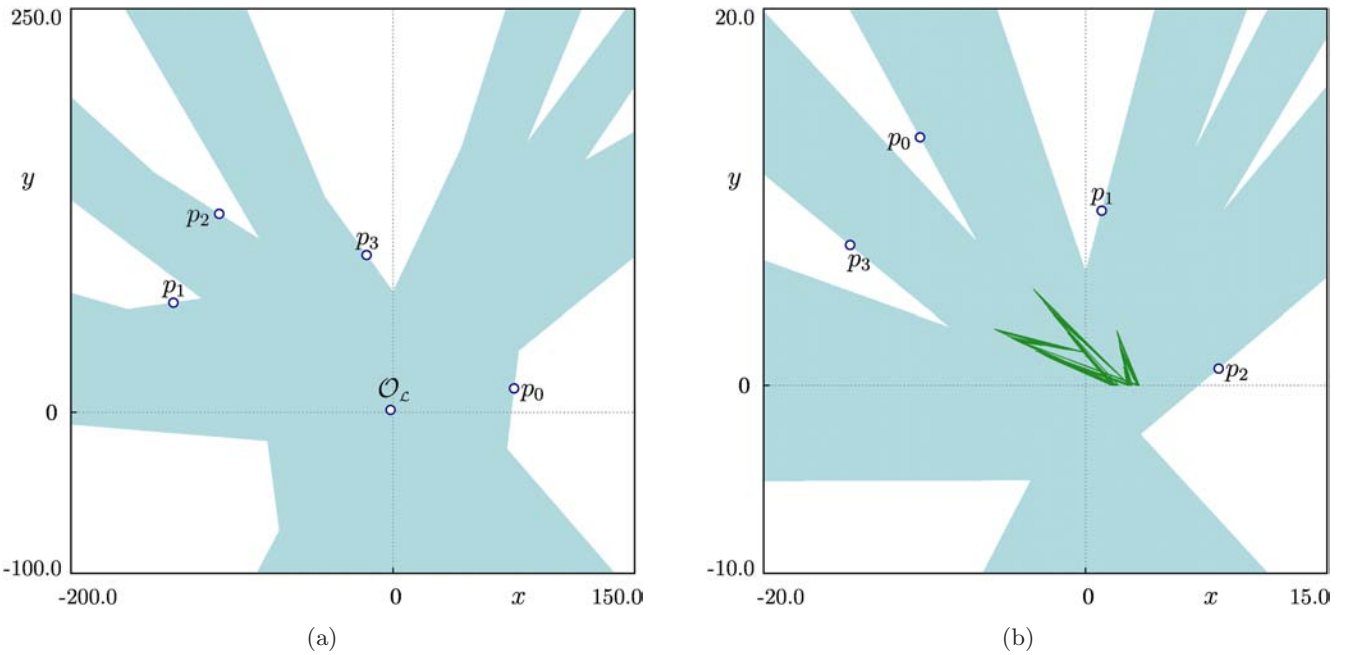

Fig. 6. Structure of the state space (a) before and (b) after a dangerous border collision bifurcation leading from a stable fixed point to a chaotic attractor. Parameters: $\tau_\mathcal{L} = 1.28$, $\tau_\mathcal{R} = -2$, $\delta_\mathcal{L} = 0.9$, $\delta_\mathcal{R} = -0.9$, (a) $\mu = -1$; (b) $\mu = 1$.

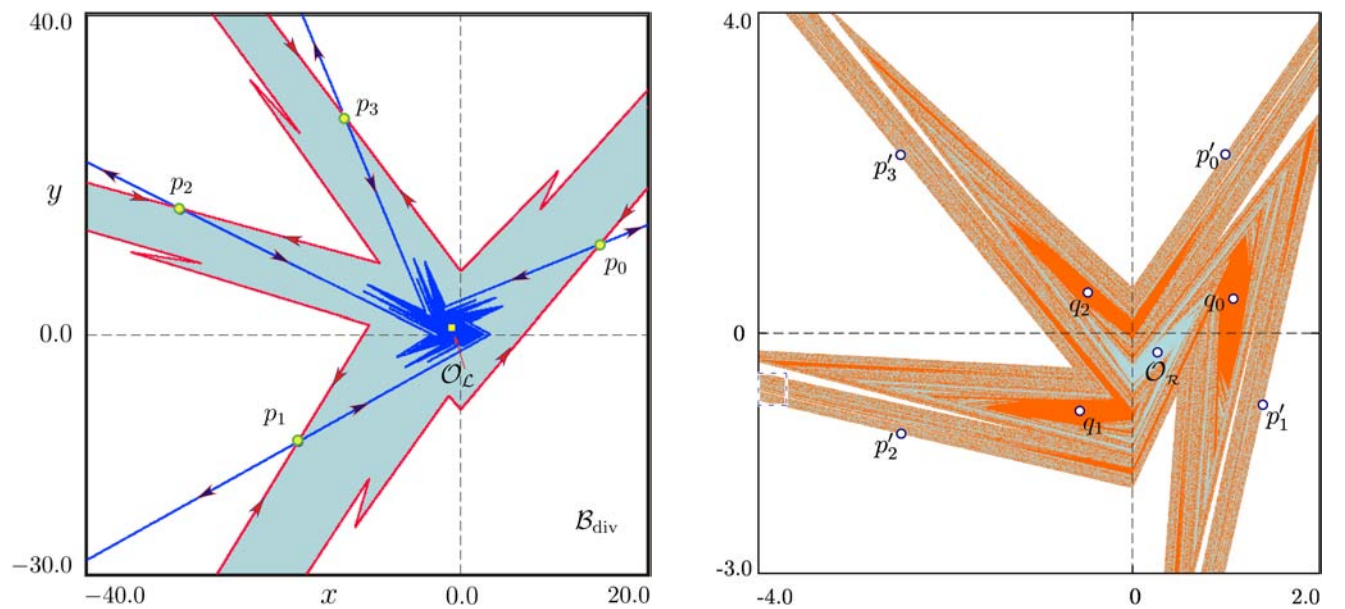

Fig. 7. Structure of the state space (a) before and (b) after a dangerous border collision bifurcation leading from a regular to a fractal boundary $\partial\mathcal{B}_{\text{div}}$. (a) Before the bifurcation, the only attractor is the fixed point $\mathcal{O}_\mathcal{L}$. The boundary $\partial\mathcal{B}_{\text{div}}$ is formed by the stable manifold of the 4-cycle $\mathcal{O}_{\mathcal{RL}^3} = \{p_0, \ldots, p_3\}$. The stable and the unstable manifolds of $\mathcal{O}_{\mathcal{RL}^3}$ are shown in red and in blue, respectively. (b) After the bifurcation, the stable fixed point $\mathcal{O}_\mathcal{R}$ and the stable 3-cycle $\mathcal{O}_{\mathcal{RL}^2} = \{q_0, q_1, q_2\}$ coexist (the basins $\mathcal{B}(\mathcal{O}_\mathcal{R})$ and $\mathcal{B}(\mathcal{O}_{\mathcal{RL}^2})$ are shown in blue and in orange, respectively). (c) Intersection of stable and unstable manifolds of the 4-cycle $\mathcal{O}_{\mathcal{R}^2\mathcal{L}^2} = \{p'_0, \ldots, p'_3\}$ (shown in red and in blue, respectively). In addition, $\mathcal{O}_\mathcal{R}$, $\mathcal{O}_{\mathcal{RL}^2}$ and the saddle 3-cycle $\mathcal{O}_{\mathcal{R}^2\mathcal{L}} = \{q'_0, q'_1, q'_2\}$ are shown. (d) Magnification of the rectangle marked in (b). Parameters: $\tau_\mathcal{L} = 0.9$, $\tau_\mathcal{R} = -1.85$, $\delta_\mathcal{L} = \delta_\mathcal{R} = 0.9$, (a) $\mu = -1$; (b)–(d) $\mu = 1$. The corresponding point in the parameter plane $(\tau_\mathcal{L}, \tau_\mathcal{R})$ is marked with D in Fig. 10.

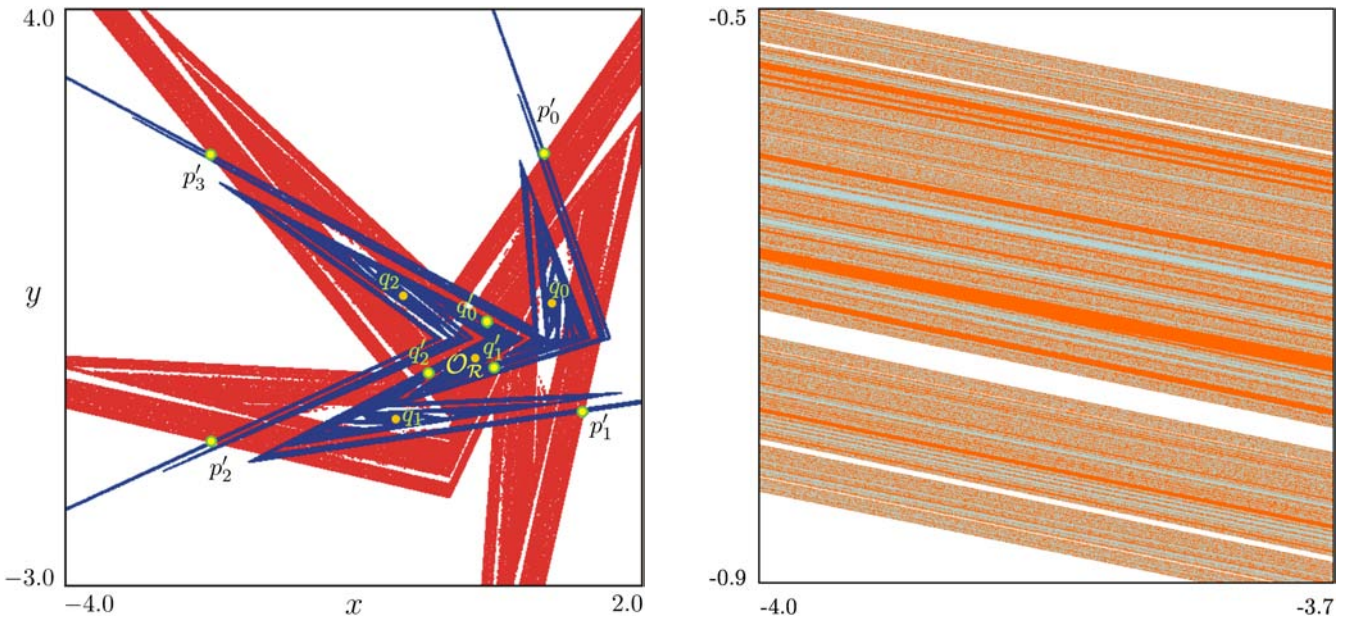

(c) (d)

Fig. 7. (*Continued*)

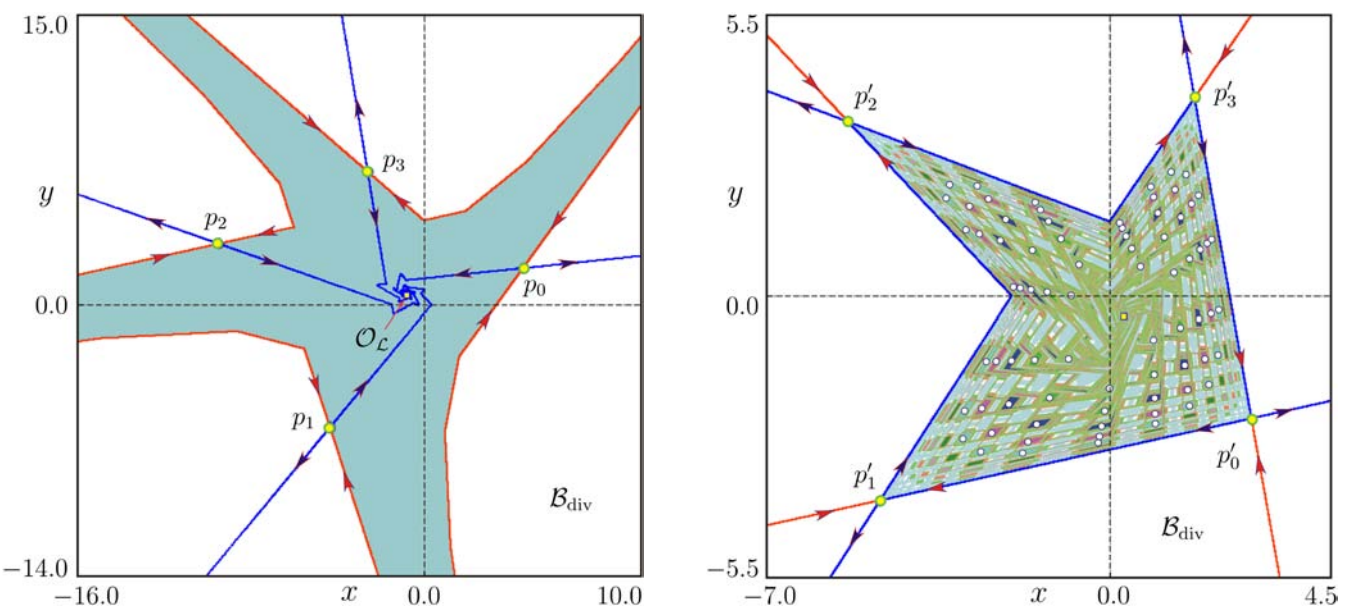

(a) (b)

Fig. 8. Structure of the state space (a) before and (b) after a dangerous border collision bifurcation leading from a stable fixed point to infinitely many attracting cycles. Parameters: $\tau_\mathcal{L} = 0.5$, $\tau_\mathcal{R} = -1.139755486$, $\delta_\mathcal{L} = 1/\delta_\mathcal{R}$, $\delta_\mathcal{R} = 1.378851759$, (a) $\mu = -1$; (b) $\mu = 1$. Notice that for $\mu > 0$ the basin boundary is formed by a closed invariant curve — a homoclinic connection between the points of a 4-cycle.

the bifurcation the fixed point $\mathcal{O}_{\mathcal{L}}$ is stable and its basin of attraction is separated from $\mathcal{B}_{\rm div}$ by the stable manifold of the saddle 4-cycle $\mathcal{O}_{\mathcal{R}\mathcal{L}^3}$. The border collision occurring at $\mu = 0$ leads a chaotic attractor to appear, with a basin of attraction separated from $\mathcal{B}_{\rm div}$ by the stable manifold of a different saddle 4-cycle, namely $\mathcal{O}_{\mathcal{R}\mathcal{L}^2\mathcal{R}}$.

Example 5. *Fixed point ↔ infinitely many attracting cycles*

It is shown in [Simpson, 2014] that map (1) may exhibit infinitely many coexisting attracting cycles. The appearance of these cycles may be associated with a dangerous bifurcation, as illustrated in Fig. 8. Before the bifurcation, there is an attracting fixed point $\mathcal{O}_{\mathcal{L}}$ and its basin boundary is given by the stable manifold of the period-4 saddle cycle $\mathcal{O}_{\mathcal{R}\mathcal{L}^3}$. After the bifurcation attracting cycles $\mathcal{O}_{(\mathcal{R}\mathcal{L}\mathcal{L}\mathcal{R})^k\mathcal{R}\mathcal{L}\mathcal{L}}$ exist for all $k \geq 1$, and the union of all their basins is separated from the divergent domain $\mathcal{B}_{\rm div}$ by a closed invariant curve formed by a homoclinic connection between points of the period-4 saddle cycle $\mathcal{O}_{\mathcal{R}\mathcal{L}\mathcal{L}\mathcal{R}}$ (see Sec. 5.2 for details).

Example 6. *Fractal basin boundary*

In the examples described so far, the unbounded boundary $\partial\mathcal{B}_{\rm div}$ of the divergent domain has a quite simple structure, but it is also possible to have $\partial\mathcal{B}_{\rm div}$ with a fractal structure [Gardini *et al.*, 2009], as illustrated in Fig. 7.

Similar to the previous examples, before the bifurcation [see Fig. 7(a)] the fixed point $\mathcal{O}_{\mathcal{L}}$ is the unique attractor and the boundary $\partial\mathcal{B}_{\rm div}$ is given by the stable manifold of the period-4 saddle cycle $\mathcal{O}_{\mathcal{R}\mathcal{L}^3}$. After the bifurcation the attracting fixed point $\mathcal{O}_{\mathcal{R}}$ coexists with the attracting 3-cycle $\mathcal{O}_{\mathcal{R}\mathcal{L}^2}$, and the boundary $\partial\mathcal{B}_{\rm div}$ has a fractal structure [see Fig. 7(b)]. In this case the boundary $\partial\mathcal{B}_{\rm div}$ includes homoclinic points which appear for example due to the intersection of stable and unstable manifolds of the singleton cycle $\mathcal{O}_{\mathcal{R}^2\mathcal{L}^2}$ as well as other homoclinic connections and heteroclinic loops [see Fig. 7(c)].

5. Types of Dangerous Bifurcations

One of the key points in the extended definition of a dangerous border collision bifurcation is the existence, before and after the bifurcation, of a domain with a positive measure associated with divergent trajectories. Divergent trajectories can be seen as trajectories converging to an attractor located at infinity. Therefore, to understand possible types of dangerous bifurcations it is necessary to identify the boundary of this domain of divergent trajectories. Then, for μ approaching zero, this boundary shrinks to the zero measure and causes a dangerous bifurcation to occur. Note that there are basically two types of boundaries:

- Type-I: Unbounded boundary $\partial\mathcal{B}_{\rm div}$,
- Type-II: Bounded boundary $\partial\mathcal{B}_{\rm div}$.

Below we take up these two cases separately.

5.1. *Unbounded boundary $\partial\mathcal{B}_{\rm div}$*

Historically, the occurrence of dangerous border collision bifurcations was first analyzed in [Ganguli & Banerjee, 2005] for the specific case that the basin of the stable fixed point extends to infinity. The standard set of parameter values considered first in [Hassouneh *et al.*, 2004] and thereafter in many other publications is $\delta_{\mathcal{L}} = \delta_{\mathcal{R}} = 0.9$. It has been shown in [Ganguli & Banerjee, 2005] that, for these parameter values, the regions of the $(\tau_{\mathcal{L}}, \tau_{\mathcal{R}})$ parameter plane for dangerous border collision bifurcation given in [Hassouneh *et al.*, 2004] can be understood by considering the basic $(k+1)$-cycles $\mathcal{O}_{\mathcal{R}\mathcal{L}^k}$ and their complementary cycles $\mathcal{O}_{\mathcal{R}\mathcal{L}^{k-1}\mathcal{R}}$. Below we briefly summarize the mechanism leading to dangerous bifurcations in this case. Note that for historical reasons the discussion below is given for basic cycles, although the same mechanism may apply to other cycles as well, both for original and extended definitions of dangerous bifurcations.

Recall that both for $\mu > 0$ and $\mu < 0$, for each $k \geq 1$ a pair of complementary $(k+1)$-cycles $\mathcal{O}_{\mathcal{R}\mathcal{L}^k}$ and $\mathcal{O}_{\mathcal{R}\mathcal{L}^{k-1}\mathcal{R}}$ appear via a border collision fold bifurcation $\xi_{\mathcal{R}\mathcal{L}^k/\mathcal{R}\mathcal{L}^{k-1}\mathcal{R}}$. For $\mu > 0$ the basic cycle $\mathcal{O}_{\mathcal{R}\mathcal{L}^k}$ may appear stable or unstable (an attracting node or a saddle), while its complementary cycle $\mathcal{O}_{\mathcal{R}\mathcal{L}^{k-1}\mathcal{R}}$ appears unstable (a saddle or a repelling node, respectively). The existence regions $\mathcal{P}^{(+)}_{\mathcal{R}\mathcal{L}^k}$ and $\mathcal{P}^{(+)}_{\mathcal{R}\mathcal{L}^{k-1}\mathcal{R}}$ (here the upper index refers to the sign of μ) are confined by the common boundary given by the border collision bifurcation curve $\xi_{\mathcal{R}\mathcal{L}^k/\mathcal{R}\mathcal{L}^{k-1}\mathcal{R}}$ and additionally by the curves $\eta_{\mathcal{R}\mathcal{L}^k}$, $\eta_{\mathcal{R}\mathcal{L}^{k-1}\mathcal{R}}$ of degenerate transcritical bifurcations of the cycles $\mathcal{O}_{\mathcal{R}\mathcal{L}^k}$ and $\mathcal{O}_{\mathcal{R}\mathcal{L}^{k-1}\mathcal{R}}$, respectively, [Sushko & Gardini, 2010], also known as Poincaré equator collisions [Avrutin *et al.*, 2010] [see Fig. 9(a)]. At these bifurcations the corresponding cycles tend to infinity and

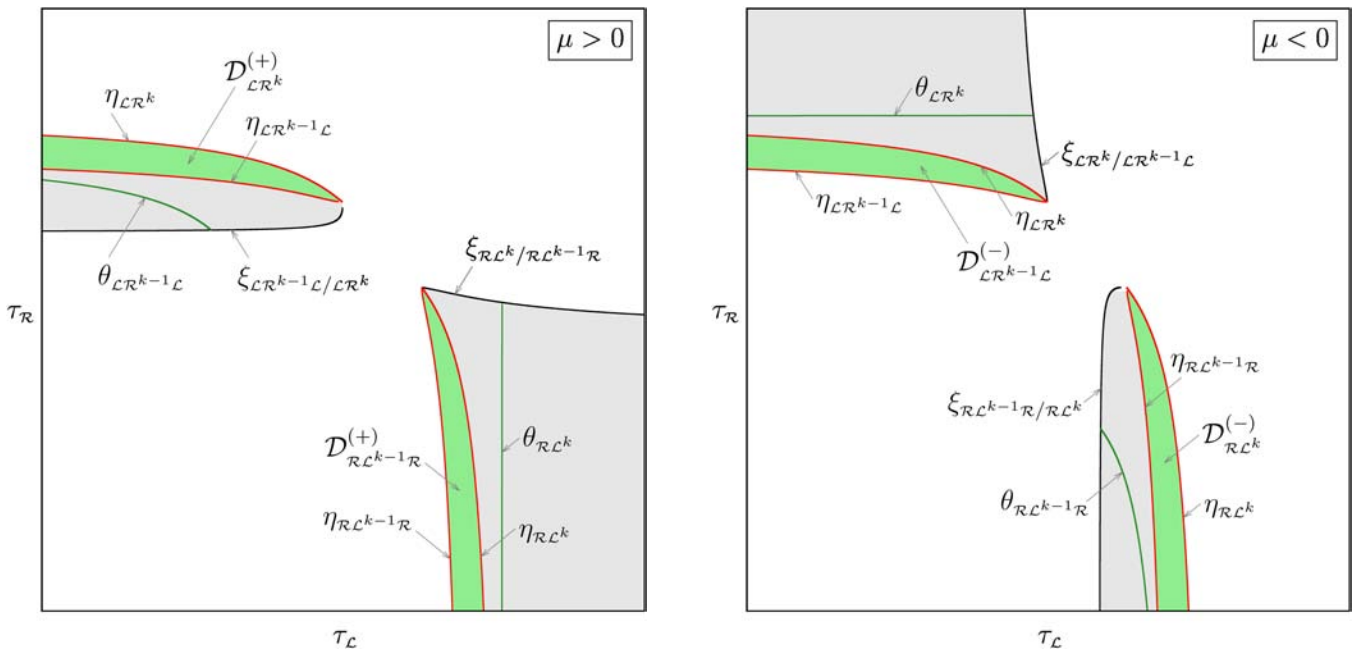

Fig. 9. Schematic representation of the regions $\mathcal{D}^{(+)}_{\mathcal{R}\mathcal{L}^{k-1}\mathcal{R}} \equiv \mathcal{D}^{(-)}_{\mathcal{R}\mathcal{L}^k}$ and $\mathcal{D}^{(+)}_{\mathcal{L}\mathcal{R}^k} \equiv \mathcal{D}^{(-)}_{\mathcal{L}\mathcal{R}^{k-1}\mathcal{L}}$ in the $(\tau_{\mathcal{L}}, \tau_{\mathcal{R}})$ parameter plane related to dangerous bifurcations for (a) $\mu > 0$ and (b) $\mu < 0$, shown in green.

disappear. It is essential for the occurrence of dangerous bifurcations related to cycles $\mathcal{O}_{\mathcal{R}\mathcal{L}^{k-1}\mathcal{R}}$ that the region of existence of $\mathcal{O}_{\mathcal{R}\mathcal{L}^k}$ is smaller than the regions of existence of $\mathcal{O}_{\mathcal{R}\mathcal{L}^{k-1}\mathcal{R}}$ [Ganguli & Banerjee, 2005], i.e. the regions $\mathcal{P}^{(+)}_{\mathcal{R}\mathcal{L}^k}$ and $\mathcal{P}^{(+)}_{\mathcal{R}\mathcal{L}^{k-1}\mathcal{R}}$ satisfy

$$\mathcal{P}^{(+)}_{\mathcal{R}\mathcal{L}^k} \subsetneq \mathcal{P}^{(+)}_{\mathcal{R}\mathcal{L}^{k-1}\mathcal{R}} \equiv \mathcal{P}^{(+),u}_{\mathcal{R}\mathcal{L}^{k-1}\mathcal{R}} \tag{6}$$

i.e. there exists a nonempty region

$$\mathcal{D}^{(+)}_{\mathcal{R}\mathcal{L}^{k-1}\mathcal{R}} = \mathcal{P}^{(+)}_{\mathcal{R}\mathcal{L}^{k-1}\mathcal{R}} \backslash \mathcal{P}^{(+)}_{\mathcal{R}\mathcal{L}^k} \tag{7}$$

in which the cycle $\mathcal{O}_{\mathcal{R}\mathcal{L}^{k-1}\mathcal{R}}$ exists, while the cycle $\mathcal{O}_{\mathcal{R}\mathcal{L}^k}$ does not. In the region $\mathcal{P}^{(+)}_{\mathcal{R}\mathcal{L}^k}$ there exists a heteroclinic connection from $\mathcal{O}_{\mathcal{R}\mathcal{L}^{k-1}\mathcal{R}}$ to $\mathcal{O}_{\mathcal{R}\mathcal{L}^k}$, i.e. an unstable manifold of the saddle cycle $\mathcal{O}_{\mathcal{R}\mathcal{L}^{k-1}\mathcal{R}}$ converges to $\mathcal{O}_{\mathcal{R}\mathcal{L}^k}$. In this case, if the cycle $\mathcal{O}_{\mathcal{R}\mathcal{L}^k}$ is not the only attractor, then the stable manifold of the saddle cycle $\mathcal{O}_{\mathcal{R}\mathcal{L}^{k-1}\mathcal{R}}$ separates the basin $\mathcal{B}(\mathcal{O}_{\mathcal{R}\mathcal{L}^k})$ from the basin of a different attractor (for example, if the parameters belong to the region $\mathcal{P}$, then this different attractor may be the stable fixed point $\mathcal{O}_{\mathcal{R}}$). As the cycle $\mathcal{O}_{\mathcal{R}\mathcal{L}^k}$ disappears after the degenerate transcritical bifurcation, an unstable manifold of the saddle cycle $\mathcal{O}_{\mathcal{R}\mathcal{L}^{k-1}\mathcal{R}}$ goes to infinity, while the stable manifold of $\mathcal{O}_{\mathcal{R}\mathcal{L}^{k-1}\mathcal{R}}$ belongs to the boundary of the divergent domain $\mathcal{B}_{\text{div}}$.

As μ passes through zero, all the cycles existing for $\mu > 0$ disappear in a nonregular border collision bifurcation at which all points of the cycle collide simultaneously with the origin. Which attracting and repelling sets appear after the bifurcation depends on the parameter values. For our purposes it is only important that for $\mu < 0$ and any $k \geq 0$ there exists again a pair of complementary $(k+1)$-cycles $\mathcal{O}_{\mathcal{R}\mathcal{L}^{k-1}\mathcal{R}}$ and $\mathcal{O}_{\mathcal{R}\mathcal{L}^k}$. As proved in Appendix A, their existence regions $\mathcal{P}^{(-)}_{\mathcal{R}\mathcal{L}^{k-1}\mathcal{R}}$ and $\mathcal{P}^{(-)}_{\mathcal{R}\mathcal{L}^k}$ differ from the existence regions $\mathcal{P}^{(+)}_{\mathcal{R}\mathcal{L}^{k-1}\mathcal{R}}$ and $\mathcal{P}^{(+)}_{\mathcal{R}\mathcal{L}^k}$ of these cycles for $\mu > 0$ but have (neglecting the sign of μ) a nonempty overlap with these regions. As for $\mu > 0$ the cycles appear via a border collision fold bifurcation $\xi_{\mathcal{R}\mathcal{L}^{k-1}\mathcal{R}/\mathcal{R}\mathcal{L}^k}$ but by contrast to the case $\mu > 0$ the cycle $\mathcal{O}_{\mathcal{R}\mathcal{L}^{k-1}\mathcal{R}}$ may appear stable or unstable, while its complementary cycle $\mathcal{O}_{\mathcal{R}\mathcal{L}^k}$ appears always unstable. Similar to the previous case, the existence regions $\mathcal{P}^{(-)}_{\mathcal{R}\mathcal{L}^{k-1}\mathcal{R}}$ and $\mathcal{P}^{(-)}_{\mathcal{R}\mathcal{L}^k}$ are confined by the common boundary $\xi_{\mathcal{R}\mathcal{L}^{k-1}\mathcal{R}/\mathcal{R}\mathcal{L}^k}$ and additionally by the degenerate transcritical bifurcation curves $\eta_{\mathcal{R}\mathcal{L}^k}$ and $\eta_{\mathcal{R}\mathcal{L}^{k-1}\mathcal{R}}$ [see Fig. 9(b)]. However, for $\mu < 0$ the regions $\mathcal{P}^{(-)}_{\mathcal{R}\mathcal{L}^{k-1}\mathcal{R}}$ and $\mathcal{P}^{(-)}_{\mathcal{R}\mathcal{L}^k}$ satisfy

$$\mathcal{P}^{(-)}_{\mathcal{R}\mathcal{L}^{k-1}\mathcal{R}} \subsetneq \mathcal{P}^{(-)}_{\mathcal{R}\mathcal{L}^k} \equiv \mathcal{P}^{(-),u}_{\mathcal{R}\mathcal{L}^k} \tag{8}$$

so that there exists a nonempty region

$$\mathcal{D}^{(-)}_{\mathcal{R}\mathcal{L}^k} = \mathcal{P}^{(-)}_{\mathcal{R}\mathcal{L}^k} \backslash \mathcal{P}^{(-)}_{\mathcal{R}\mathcal{L}^{k-1}\mathcal{R}} \tag{9}$$

in which the unstable cycle $\mathcal{O}_{\mathcal{RL}^k}$ exists and the cycle $\mathcal{O}_{\mathcal{RL}^{k-1}\mathcal{R}}$ does not. Moreover, as proved in Appendix A, the shapes of the regions $\mathcal{D}^{(+)}_{\mathcal{RL}^{k-1}\mathcal{R}}$ and $\mathcal{D}^{(-)}_{\mathcal{RL}^k}$ coincide, i.e. for all $\mu > 0$

$$(\tau_{\mathcal{L}/\mathcal{R}}, \delta_{\mathcal{L}/\mathcal{R}}, \mu) \in \mathcal{D}^{(+)}_{\mathcal{RL}^{k-1}\mathcal{R}} \Leftrightarrow (\tau_{\mathcal{L}/\mathcal{R}}, \delta_{\mathcal{L}/\mathcal{R}}, -\mu) \in \mathcal{D}^{(-)}_{\mathcal{RL}^k}. \quad (10)$$

Therefore, for the values of $\tau_{\mathcal{L}/\mathcal{R}}$, $\delta_{\mathcal{L}/\mathcal{R}}$ belonging to these regions the condition (ii) is satisfied both for $\mu < 0$ and $\mu > 0$. Accordingly, if the condition (i) is satisfied as well, then the variation of μ through zero at these values of $\tau_{\mathcal{L}/\mathcal{R}}$, $\delta_{\mathcal{L}/\mathcal{R}}$ leads to a dangerous bifurcation.

In addition to the stability regions $\mathcal{P}^{(+)}_{\mathcal{RL}^k}$, for $\mu > 0$ there exists a sequence of regions in which the cycles $\mathcal{O}_{\mathcal{LR}^{k-1}\mathcal{L}}$ are stable. These cycles appear at a border collision fold bifurcation $\xi_{\mathcal{LR}^{k-1}\mathcal{L}/\mathcal{LR}^k}$ together with the cycles $\mathcal{O}_{\mathcal{LR}^k}$ which are unstable everywhere [see Fig. 9(a)]. Similar to the cycles described above, the existence regions are confined by the curves of degenerate transcritical bifurcations $\eta_{\mathcal{LR}^{k-1}\mathcal{L}}$ and $\eta_{\mathcal{LR}^k}$, respectively, at which the corresponding cycles tend to infinity and disappear. The regions satisfy

$$\mathcal{P}^{(+)}_{\mathcal{LR}^{k-1}\mathcal{L}} \subsetneq \mathcal{P}^{(+)}_{\mathcal{LR}^k} \equiv \mathcal{P}^{(+),u}_{\mathcal{LR}^k} \quad (11)$$

so that in the nonempty region

$$\mathcal{D}^{(+)}_{\mathcal{LR}^k} = \mathcal{P}^{(+)}_{\mathcal{LR}^k} \backslash \mathcal{P}^{(+)}_{\mathcal{LR}^{k-1}\mathcal{L}} \quad (12)$$

the cycle $\mathcal{O}_{\mathcal{LR}^{k-1}\mathcal{L}}$ does not exist and the unstable manifold of the saddle cycle $\mathcal{O}_{\mathcal{LR}^k}$ goes to infinity. Similarly, for $\mu < 0$ there exists a sequence of regions $\mathcal{P}^{(-)}_{\mathcal{LR}^k}$ and $\mathcal{P}^{(-)}_{\mathcal{LR}^{k-1}\mathcal{L}}$ associated with cycles $\mathcal{O}_{\mathcal{LR}^k}$ (which may appear stable or unstable) and $\mathcal{O}_{\mathcal{LR}^{k-1}\mathcal{L}}$ (which appears unstable). The regions satisfy

$$\mathcal{P}^{(-)}_{\mathcal{LR}^k} \subsetneq \mathcal{P}^{(-)}_{\mathcal{LR}^{k-1}\mathcal{L}} \equiv \mathcal{P}^{(-),u}_{\mathcal{LR}^{k-1}\mathcal{L}} \quad (13)$$

which gives rise to the nonempty region

$$\mathcal{D}^{(-)}_{\mathcal{LR}^{k-1}\mathcal{L}} = \mathcal{P}^{(-)}_{\mathcal{LR}^{k-1}\mathcal{L}} \backslash \mathcal{P}^{(-)}_{\mathcal{LR}^k}. \quad (14)$$

As before, the shapes of the regions $\mathcal{D}^{(+)}_{\mathcal{LR}^k}$ and $\mathcal{D}^{(-)}_{\mathcal{LR}^{k-1}\mathcal{L}}$ coincide, i.e. for all $\mu > 0$

$$(\tau_{\mathcal{L}/\mathcal{R}}, \delta_{\mathcal{L}/\mathcal{R}}, \mu) \in \mathcal{D}^{(+)}_{\mathcal{LR}^k} \Leftrightarrow (\tau_{\mathcal{L}/\mathcal{R}}, \delta_{\mathcal{L}/\mathcal{R}}, -\mu) \in \mathcal{D}^{(-)}_{\mathcal{LR}^{k-1}\mathcal{L}} \quad (15)$$

so that if the values of $\tau_{\mathcal{L}/\mathcal{R}}$, $\delta_{\mathcal{L}/\mathcal{R}}$ belong to these regions and the condition (i) is satisfied then the variation of μ through zero at these values of $\tau_{\mathcal{L}/\mathcal{R}}$, $\delta_{\mathcal{L}/\mathcal{R}}$ lead to a dangerous bifurcation. Together with Eq. (10), Eq. (15) is proved in Appendix A.

An analytic calculation of the boundaries of the regions $\mathcal{D}^{(+)}_{\mathcal{RL}^{k-1}\mathcal{R}} \equiv \mathcal{D}^{(-)}_{\mathcal{RL}^k}$ and $\mathcal{D}^{(+)}_{\mathcal{LR}^k} \equiv \mathcal{D}^{(-)}_{\mathcal{LR}^{k-1}\mathcal{L}}$ can easily be done for any k, in particular using recently developed technique reported in [Saha & Banerjee, 2016] (a brief description is given in Appendix B).

Figure 10 presents the structure of the $(\tau_{\mathcal{L}}, \tau_{\mathcal{R}})$ parameter plane at $\delta_{\mathcal{L}} = \delta_{\mathcal{R}} = 0.9$ for $\mu > 0$ and $\mu < 0$, showing regions in which condition (i) [Figs. 10(a) and 10(b)] and condition (ii) [Fig. 10(c)] are satisfied. Examples for the above mentioned regions $\mathcal{D}^{(+)}_{\mathcal{RL}^{k-1}\mathcal{R}} \equiv \mathcal{D}^{(-)}_{\mathcal{LR}^{k-1}\mathcal{L}}$ and $\mathcal{D}^{(+)}_{\mathcal{LR}^k} \equiv \mathcal{D}^{(-)}_{\mathcal{RL}^k}$ are marked in Fig. 10(c). As one can see in this figure, in addition to the regions, there are several other regions in the $(\tau_{\mathcal{L}}, \tau_{\mathcal{R}})$ parameter plane for which divergent behavior exists. To explain their appearance, consider as an example, the sequence of regions $\mathcal{P}^{(+)}_{(\mathcal{RL})^k\mathcal{RL}^2}$ marked in Fig. 10(a). In the same way as the regions $\mathcal{P}^{(+)}_{\mathcal{RL}^k}$ described above, these regions are confined by two bifurcation boundaries, one associated with a fold border collision bifurcation $\xi_{(\mathcal{RL})^k\mathcal{RL}^2/(\mathcal{RL})^k\mathcal{R}^2\mathcal{L}}$, and the other one with degenerate transcritical bifurcation $\eta_{(\mathcal{RL})^k\mathcal{RL}^2}$. Similarly, in Fig. 10(b) the regions $\mathcal{P}^{(-)}_{(\mathcal{RL})^k\mathcal{R}^2\mathcal{L}}$ are marked, confined by the fold border collision bifurcation boundary $\xi_{(\mathcal{RL})^k\mathcal{R}^2\mathcal{L}/(\mathcal{RL})^k\mathcal{RL}^2}$, and the degenerate transcritical bifurcation boundary $\eta_{(\mathcal{RL})^k\mathcal{R}^2\mathcal{L}}$. As a consequence, we observe a sequence of regions $\mathcal{D}^{(+)}_{(\mathcal{RL})^k\mathcal{R}^2\mathcal{L}} \equiv \mathcal{D}^{(-)}_{(\mathcal{RL})^k\mathcal{RL}^2}$ confined (both for $\mu > 0$ and for $\mu < 0$) by the degenerate transcritical bifurcation boundaries and their shapes coincide in the same way as for the regions $\mathcal{D}^{(+)}_{\mathcal{RL}^{k-1}\mathcal{R}} \equiv \mathcal{D}^{(-)}_{\mathcal{LR}^{k-1}\mathcal{L}}$, as proved in Appendix A. In these regions, if some attractors exist both for $\mu > 0$ and $\mu < 0$, then they are associated with dangerous bifurcations.

Note also that not every region associated with a stable cycle shown in Fig. 10(a) is accompanied by the corresponding dangerous region. For example, at the considered parameter values the boundaries of the regions $\mathcal{P}^{(+)}_{\mathcal{R}^2\mathcal{L}^2}$ and $\mathcal{P}^{(+)}_{\mathcal{R}^2\mathcal{L}^3}$ marked in Fig. 10(a) are not associated with degenerate transcritical bifurcations, so that no dangerous regions appear. However, for other parameter values a boundary associated with a degenerate transcritical bifurcation and the associated dangerous region may appear [see the region $\mathcal{D}^{(+)}_{\mathcal{R}^3\mathcal{L}^2} \equiv \mathcal{D}^{(-)}_{\mathcal{R}^2\mathcal{L}^3}$ in Fig. 11(a)].

As one can see in Fig. 10(c), many other dangerous regions exist outside the region $\mathcal{P}$ given in

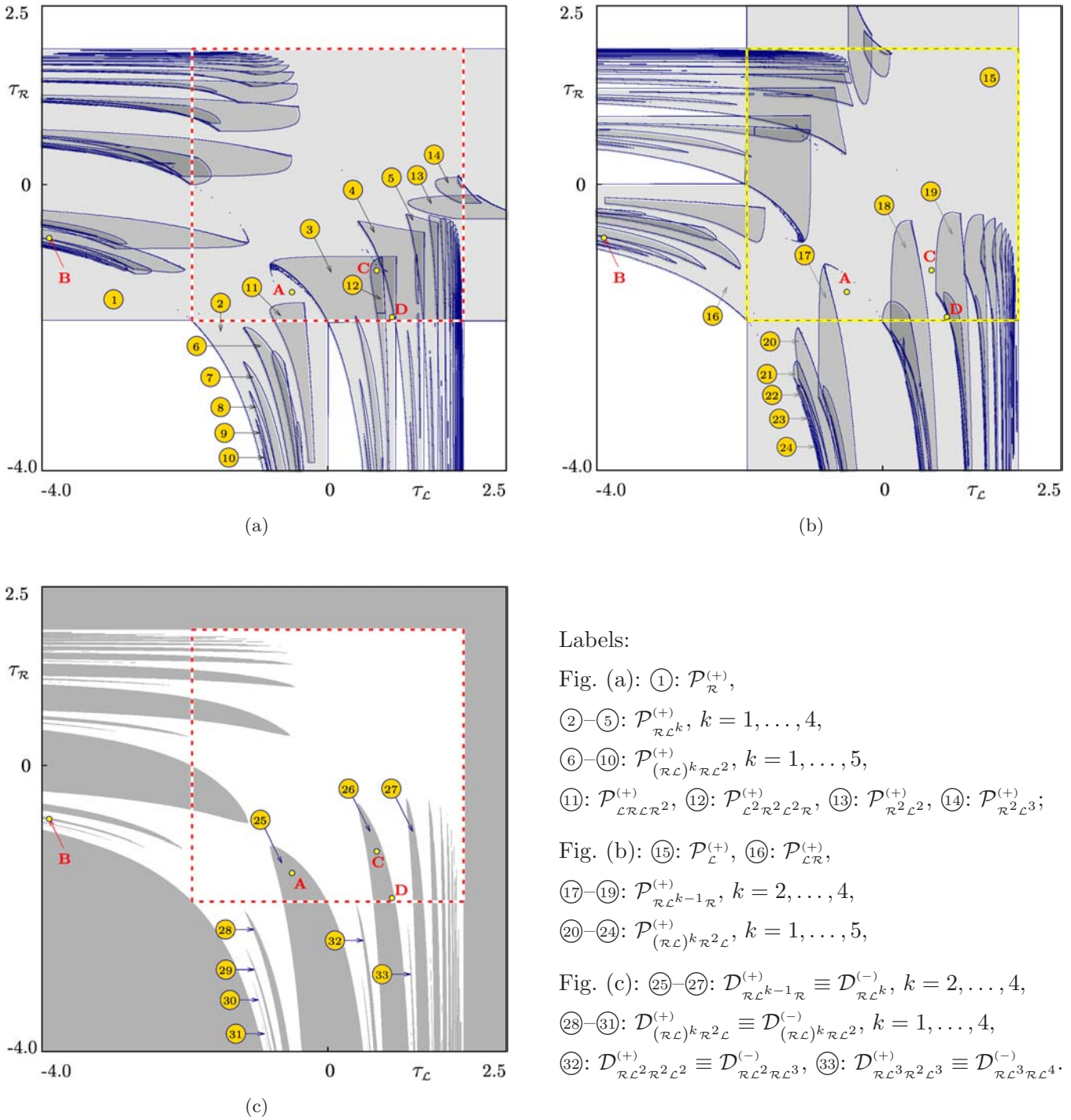

Labels:

Fig. (a): ①: $\mathcal{P}^{(+)}_{\mathcal{R}}$,

②–⑤: $\mathcal{P}^{(+)}_{\mathcal{R}\mathcal{L}^k}$, $k = 1, \ldots, 4$,

⑥–⑩: $\mathcal{P}^{(+)}_{(\mathcal{R}\mathcal{L})^k\mathcal{R}\mathcal{L}^2}$, $k = 1, \ldots, 5$,

⑪: $\mathcal{P}^{(+)}_{\mathcal{L}\mathcal{R}\mathcal{L}\mathcal{R}^2}$, ⑫: $\mathcal{P}^{(+)}_{\mathcal{L}^2\mathcal{R}^2\mathcal{L}^2\mathcal{R}}$, ⑬: $\mathcal{P}^{(+)}_{\mathcal{R}^2\mathcal{L}^2}$, ⑭: $\mathcal{P}^{(+)}_{\mathcal{R}^2\mathcal{L}^3}$;

Fig. (b): ⑮: $\mathcal{P}^{(+)}_{\mathcal{L}}$, ⑯: $\mathcal{P}^{(+)}_{\mathcal{L}\mathcal{R}}$,

⑰–⑲: $\mathcal{P}^{(+)}_{\mathcal{R}\mathcal{L}^{k-1}\mathcal{R}}$, $k = 2, \ldots, 4$,

⑳–㉔: $\mathcal{P}^{(+)}_{(\mathcal{R}\mathcal{L})^k\mathcal{R}^2\mathcal{L}}$, $k = 1, \ldots, 5$,

Fig. (c): ㉕–㉗: $\mathcal{D}^{(+)}_{\mathcal{R}\mathcal{L}^{k-1}\mathcal{R}} \equiv \mathcal{D}^{(-)}_{\mathcal{R}\mathcal{L}^k}$, $k = 2, \ldots, 4$,

㉘–㉛: $\mathcal{D}^{(+)}_{(\mathcal{R}\mathcal{L})^k\mathcal{R}^2\mathcal{L}} \equiv \mathcal{D}^{(-)}_{(\mathcal{R}\mathcal{L})^k\mathcal{R}\mathcal{L}^2}$, $k = 1, \ldots, 4$,

㉜: $\mathcal{D}^{(+)}_{\mathcal{R}\mathcal{L}^2\mathcal{R}^2\mathcal{L}^2} \equiv \mathcal{D}^{(-)}_{\mathcal{R}\mathcal{L}^2\mathcal{R}\mathcal{L}^3}$, ㉝: $\mathcal{D}^{(+)}_{\mathcal{R}\mathcal{L}^3\mathcal{R}^2\mathcal{L}^3} \equiv \mathcal{D}^{(-)}_{\mathcal{R}\mathcal{L}^3\mathcal{R}\mathcal{L}^4}$.

Fig. 10. Regions in the $(\tau_{\mathcal{L}}, \tau_{\mathcal{R}})$ parameter plane for (a) $\mu > 0$ and (b) $\mu < 0$ associated with bounded attractors. Gray scales correspond to the number of attractors (in the white regions there are no attractors, in the light gray regions only one attractor, and so on). In (c) regions with divergent behavior are shown (both for $\mu > 0$ and $\mu < 0$). Parameters: $\delta_{\mathcal{L}} = \delta_{\mathcal{R}} = 0.9$.

Eq. (3). Such regions have not been considered in [Ganguli & Banerjee, 2005], as at the parameter values considered in this work they do not intersect the region $\mathcal{P}$ and hence do not fulfill the original definition of a dangerous border collision bifurcation. However, they may fulfill the extended definition and be associated with dangerous bifurcations. An example for that has been discussed in Sec. 4 (see Example 3, Fig. 5), the corresponding point in the $(\tau_{\mathcal{L}}, \tau_{\mathcal{R}})$ parameter plane is marked with B in Fig. 10. Moreover, for increasing values of $\delta_{\mathcal{L}/\mathcal{R}}$ these regions enter the region $\mathcal{P}$, so that the original

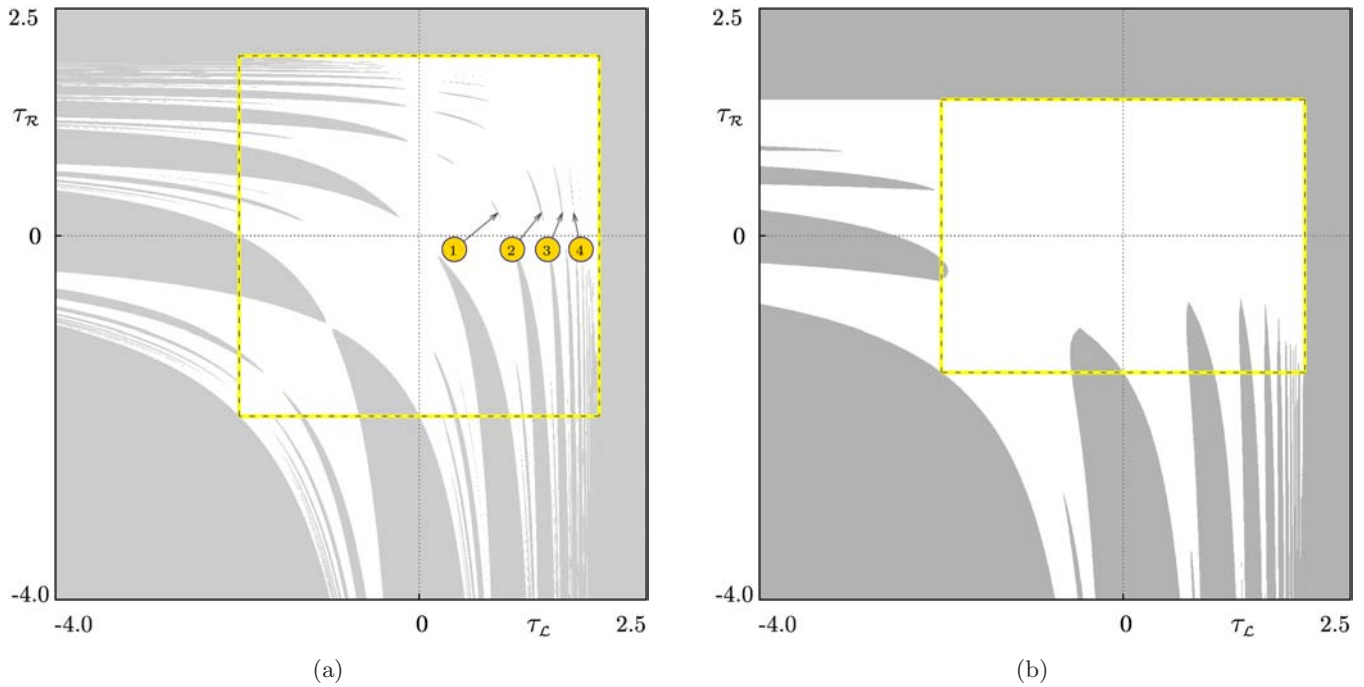

Fig. 11. Regions in the $(\tau_{\mathcal{L}}, \tau_{\mathcal{R}})$ parameter plane associated with divergent behavior (both for $\mu > 0$ and $\mu < 0$) at (a) $\delta_{\mathcal{L}} = \delta_{\mathcal{R}} = 0.98$ and (b) $\delta_{\mathcal{L}} = 0.999$, $\delta_{\mathcal{R}} = 0.5$. In (a), the regions $\mathcal{D}^{(+)}_{\mathcal{R}^3\mathcal{L}^{k-1}} \equiv \mathcal{D}^{(-)}_{\mathcal{R}^2\mathcal{L}^k}$, $k = 3, \ldots, 6$, are labeled with ①–④, respectively.

definition of a dangerous border collision bifurcation becomes fulfilled as well [see Fig. 11(a) for an example].

Even at the parameter values considered in [Ganguli & Banerjee, 2005], dangerous bifurcations occurring inside the region $\mathcal{P}$ may be associated with more complex behavior than described in the previous publications. In particular, depending on the actual parameter values one or more stability regions of cycles coexisting with stable fixed points may overlap inside $\mathcal{P}$ and intersect some of the $\mathcal{D}$-regions. As an example, one can consider the point inside the region $\mathcal{P}$ marked with C in Fig. 10 ($\tau_{\mathcal{L}} = 0.6847$, $\tau_{\mathcal{R}} = -1.196$). When μ is varied through zero at these parameter values, a dangerous bifurcation occurs and leads from the stable fixed point $\mathcal{O}_{\mathcal{L}}$ not only to the stable fixed point $\mathcal{O}_{\mathcal{R}}$ but also the stable 3-cycle $\mathcal{O}_{\mathcal{R}\mathcal{L}^2}$ and the stable 7-cycle $\mathcal{O}_{\mathcal{L}^2\mathcal{R}^2\mathcal{L}^2\mathcal{R}}$. Indeed, it can be seen in Fig. 10 that for $\mu < 0$ this point belongs to the intersection of the regions $\mathcal{D}^{(-)}_{\mathcal{R}\mathcal{L}^3}$ and $\mathcal{P}_{\mathcal{L}}$ while for $\mu > 0$ it belongs to the intersection of the regions $\mathcal{D}^{(+)}_{\mathcal{R}\mathcal{L}^2\mathcal{R}}$, $\mathcal{P}_{\mathcal{R}}$, $\mathcal{P}_{\mathcal{R}\mathcal{L}^2}$, and $\mathcal{P}_{\mathcal{L}^2\mathcal{R}^2\mathcal{L}^2\mathcal{R}}$.

It is worth noticing that for increasing values of $\delta_{\mathcal{L}}$ and $\delta_{\mathcal{R}}$, more and more regions which can lead to dangerous bifurcations appear and also enter the region $\mathcal{P}$ (so that not only the extended but also the original definition is satisfied). To give an example, Fig. 11(a) shows these regions for $\delta_{\mathcal{L}} = \delta_{\mathcal{R}} = 0.98$ and $\mu > 0$. In addition to the regions already described for $\delta_{\mathcal{L}} = \delta_{\mathcal{R}} = 0.9$, inside the region $\mathcal{P}$ one can observe the regions $\mathcal{D}^{(+)}_{\mathcal{R}^3\mathcal{L}^k} \equiv \mathcal{D}^{(-)}_{\mathcal{R}^2\mathcal{L}^{k+1}}$, $k = 2, 3, 4, 5$.

Note also that the symmetry of the regions related to dangerous bifurcations with respect to the diagonal $\tau_{\mathcal{L}} = \tau_{\mathcal{R}}$ in the examples shown above is caused by the particular setting $\delta_{\mathcal{L}} = \delta_{\mathcal{R}}$ used in these examples. Figure 11(b) illustrates that this symmetry is broken for $\delta_{\mathcal{L}} \neq \delta_{\mathcal{R}}$.

Note also that Example 5 in Sec. 4 (Fig. 8) presents a peculiar case that falls between Type-I and Type-II. For $\mu < 0$ the situation is similar to the cases shown above. The stable set of a saddle 4-cycle forms the basin boundary of the attracting fixed point $\mathcal{O}_{\mathcal{L}}$. But for $\mu > 0$ [Fig. 8(b)] the basin boundary includes a homoclinic connection between points of a single saddle 4-cycle. This is a closed invariant curve, and so it has some resemblance with Type-II. At $\mu = 0$, the basin of attraction shrinks to a set of measure zero. But the stable set of the 4-cycle (shown in red) extends to infinity which is similar to Type-I.

However, as mentioned in [Simpson, 2014], the structure of the phase space is not robust in this

case, and a generic parameter perturbation destroys the homoclinic connection, leading either to an attractor with a basin extending to infinity, or to the absence of any attractor. However, a repelling closed invariant curve at the boundary of the divergent domain may also be robust. In such a case it may be formed by a heteroclinic connection between a saddle and a repelling focus (or repelling node), or, alternatively, it can also be associated with quasiperiodic dynamics. This leads to the Type-II situation, which is described in the next section.

5.2. *Bounded boundaries $\partial\mathcal{B}_{\rm div}$*

In the situations described above, the basin of the actual attractor extends to infinity because the stable manifold of the saddle cycle forming its boundary originates from infinity. However, it is also possible that this manifold originates from a different repelling cycle (saddle or focus), forming a repelling closed invariant curve. Moreover, such a repelling closed invariant curve may also be associated with quasiperiodic dynamics. Such curves may separate the basin of attraction of the actual attractor (or attractors) from the divergent domain $\mathcal{B}_{\rm div}$, leading to dangerous bifurcations.

We now illustrate it with a few examples.

Example 7. *Closed invariant curves*

Let us consider an example of a dangerous bifurcation for which the basin of attraction of a stable motion is separated from the divergent domain $\mathcal{B}_{\rm div}$ by a repelling closed invariant curve.

For $\mu < 0$ the stable fixed point $\mathcal{O}_{\mathcal{L}}$ is surrounded by a repelling closed invariant curve that is formed by a saddle 23-cycle $\mathcal{O}_{\mathcal{L}\mathcal{R}^2\mathcal{L}\mathcal{R}^2(\mathcal{L}^2\mathcal{R}^2)^4\mathcal{L}}$ and a repelling 23-focus $\mathcal{O}_{\mathcal{R}^3\mathcal{L}\mathcal{R}^2(\mathcal{L}^2\mathcal{R}^2)^4\mathcal{L}}$ and the stable manifolds of the saddle [see Fig. 12(a)]. Similar to the examples discussed before, the stable manifold of the period-23 saddle cycle separates the basin of attraction of the stable fixed point $\mathcal{O}_{\mathcal{L}}$ from $\mathcal{B}_{\rm div}$, while the unstable manifolds W^U_-, W^U_+ of the saddle either converge on the attractor or approach infinity.

As discussed in detail below, for $\mu > 0$ the structure of the phase space is different [see Fig. 12(b)]. The fixed point $\mathcal{O}_{\mathcal{R}}$ now is a repelling focus and around it there is an attracting closed invariant curve formed by a saddle-focus connection between a saddle 4-cycle $\mathcal{O}_{\mathcal{L}\mathcal{R}^3}$ and the attracting focus $\mathcal{O}_{\mathcal{L}^2\mathcal{R}^2}$. In this case, the basin of attraction of this attractor is separated from $\mathcal{B}_{\rm div}$ by a repelling closed invariant curve associated with (numerically observed) quasiperiodic dynamics, since no cycles seem to exist outside this curve. Accordingly, as

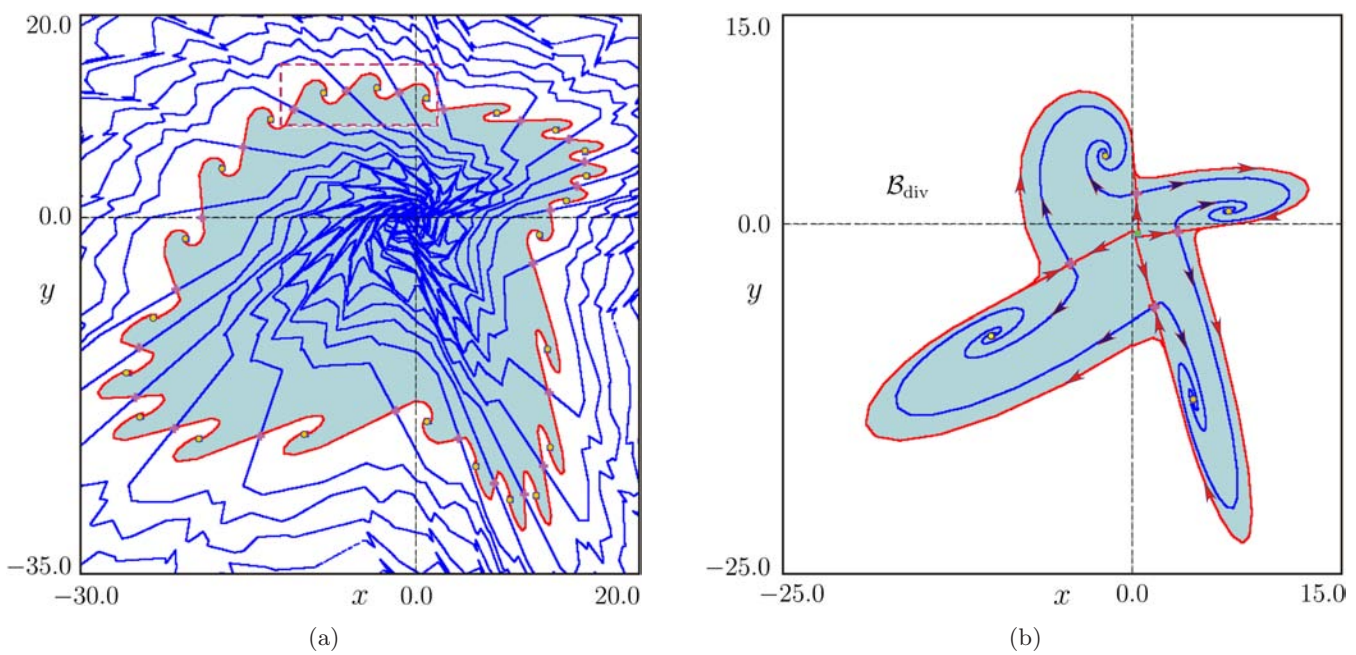

Fig. 12. Structure of the state space (a) before and (b) after a dangerous border collision bifurcation leading from a stable fixed point to a stable 4-cycle. Before and after the bifurcation the basin boundaries are bounded. In (a) the basin boundary is a closed invariant curve formed by a saddle-repelling focus connection. In (b) the closed invariant curve at the basin boundary is associated with quasiperiodic dynamics. Parameters: $\tau_{\mathcal{L}} = -0.5$, $\tau_{\mathcal{R}} = 0.35$, $\delta_{\mathcal{L}} = 0.5$, $\delta_{\mathcal{R}} = 1.8$, (a) $\mu = -1$; (b) $\mu = 1$.

μ is varied through zero, a dangerous bifurcation occurs, whereby the basin is bounded before and after the bifurcation, but the dynamics at the basin boundary differ.

Appearance of a pair of closed invariant curves

The question may arise regarding the mechanism leading to the appearance of a pair of closed invariant curves mentioned above. Indeed, often a pair of closed invariant curves appear simultaneously, one attracting and one repelling. In our case the mechanism leading to the appearance of the pair of closed invariant curves is similar to homoclinic tangles, as often occurs in two-dimensional maps, see e.g. [Foroni & Agliari, 2011; Zhusubaliyev & Mosekilde, 2015]. The main steps of this mechanism are illustrated in Figs. 13–17 when we change the value of $\tau_{\mathcal{R}}$ from $\tau_{\mathcal{R}} = 0.33$ to $\tau_{\mathcal{R}} = 0.35$. Figure 18 gives schematic diagrams to explain the succession of events.

Figure 13 shows the phase portrait of the map for $\tau_{\mathcal{R}} = 0.33$, where a stable focus $\mathcal{O}_{\mathcal{L}^2\mathcal{R}^2}$ and a saddle 4-cycle $\mathcal{O}_{\mathcal{L}\mathcal{R}^3}$ coexist with a repelling fixed point $\mathcal{O}_{\mathcal{R}}$. The stable manifold $W^S_{\pm}$ of the saddle 4-cycle forms a saddle-repelling focus connection around the periodic points of the stable focus 4-cycle and separates the basin of attraction $\mathcal{B}(\mathcal{O}_{\mathcal{L}^2\mathcal{R}^2})$ of the stable 4-cycle from the divergent domain $\mathcal{B}_{\rm div}$. As illustrated in Figs. 13 and 18(a), the branches W^U_- of the unstable manifold of the saddle cycle converge to the stable focus 4-cycle, and the others W^U_+ diverge to infinity.

As $\tau_{\mathcal{R}}$ increased, the homoclinic bifurcation (or a homoclinic contact) occurs which is similar to a homoclinic tangency in smooth maps. Figures 14 and 18(b) show the phase portrait of the map near the first homoclinic bifurcation. After this bifurcation the stable $W^S_{\pm}$ and unstable $W^U_{\pm}$ manifolds of the saddle 4-cycle intersect transversely forming a homoclinic structure [see Figs. 15 and 18(c)]. Note that the transversal homoclinic structure exists in a very narrow parameter region confined by two homoclinic bifurcation boundaries [Kuznetsov, 2004] corresponding to collisions between stable and unstable invariant manifolds from opposite sides in the phase plane. The phase portrait in Fig. 14 corresponds to the "first homoclinic contact" boundary.

As the parameter $\tau_{\mathcal{R}}$ increases, the second homoclinic bifurcation occurs. At this bifurcation the unstable manifolds $W^U_{\pm}$ of the saddle 4-cycle

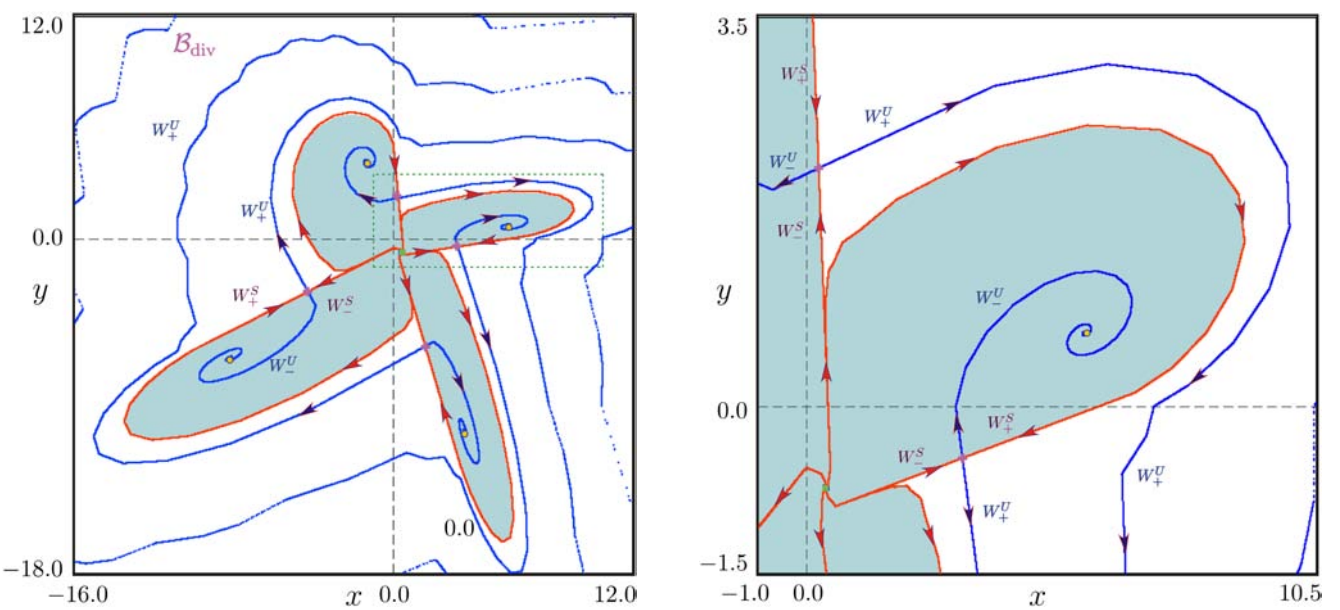

(a) (b)

Fig. 13. Structure of the state space before the first homoclinic bifurcation. A stable focus and a saddle 4-cycle coexist with a repelling fixed point. The stable manifold $W^S_{\pm}$ of the saddle cycle forms a saddle-repelling focus connection around the periodic points of the stable focus 4-cycle and separates the basin of attraction of the stable cycle from the divergent domain. The branches W^U_- of the unstable manifold of the saddle cycle converge to the stable focus 4-cycle, while the branches W^U_+ diverge to infinity. Schematically this structure is shown in Fig. 18(a). The area marked by a rectangle in (a) is shown magnified in (b). Parameters: $\tau_{\mathcal{L}} = -0.5$, $\tau_{\mathcal{R}} = 0.33$, $\delta_{\mathcal{L}} = 0.5$, $\delta_{\mathcal{R}} = 1.8$, $\mu = 1$.

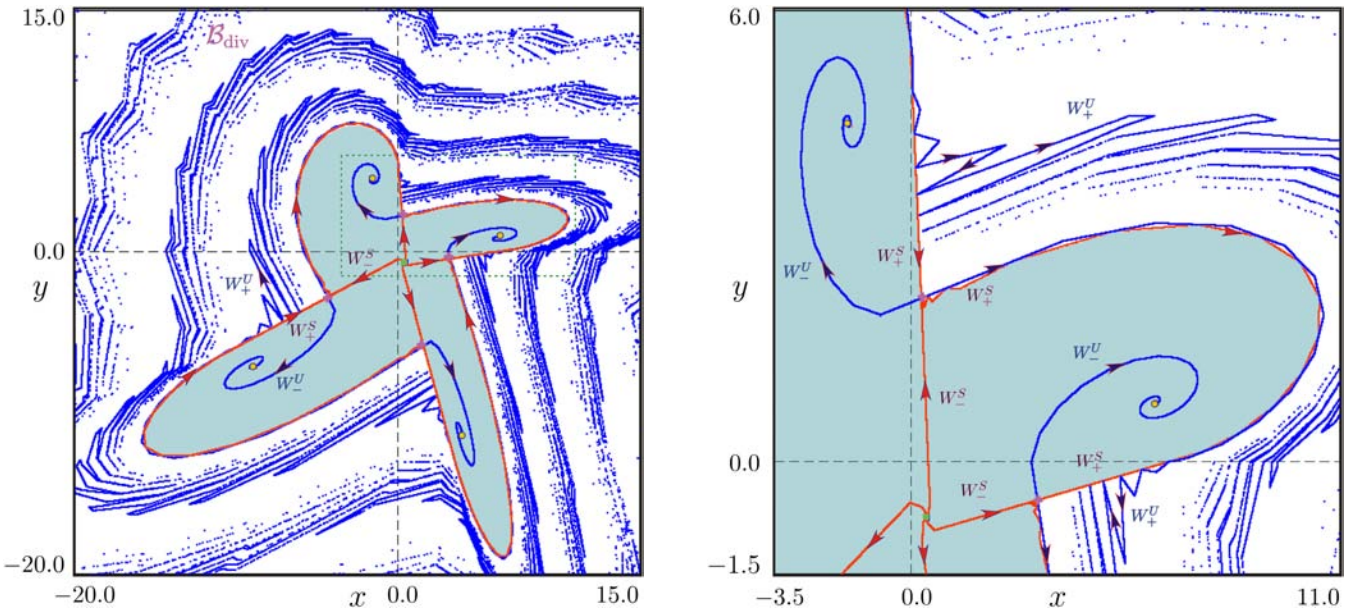

Fig. 14. Structure of the state space close to the first homoclinic bifurcation. At this bifurcation, the branches W^S_+ of the stable manifold of the saddle cycle are touched "from outside" by the branches W^U_+ of the unstable manifold (similarly to a homoclinic tangency in smooth maps). Schematically this structure is shown in Fig. 18(b). The area marked by a rectangle in (a) is shown magnified in (b). Parameters: $\tau_{\mathcal{L}} = -0.5$, $\tau_{\mathcal{R}} = 0.3385$, $\delta_{\mathcal{L}} = 0.5$, $\delta_{\mathcal{R}} = 1.8$, $\mu = 1$.

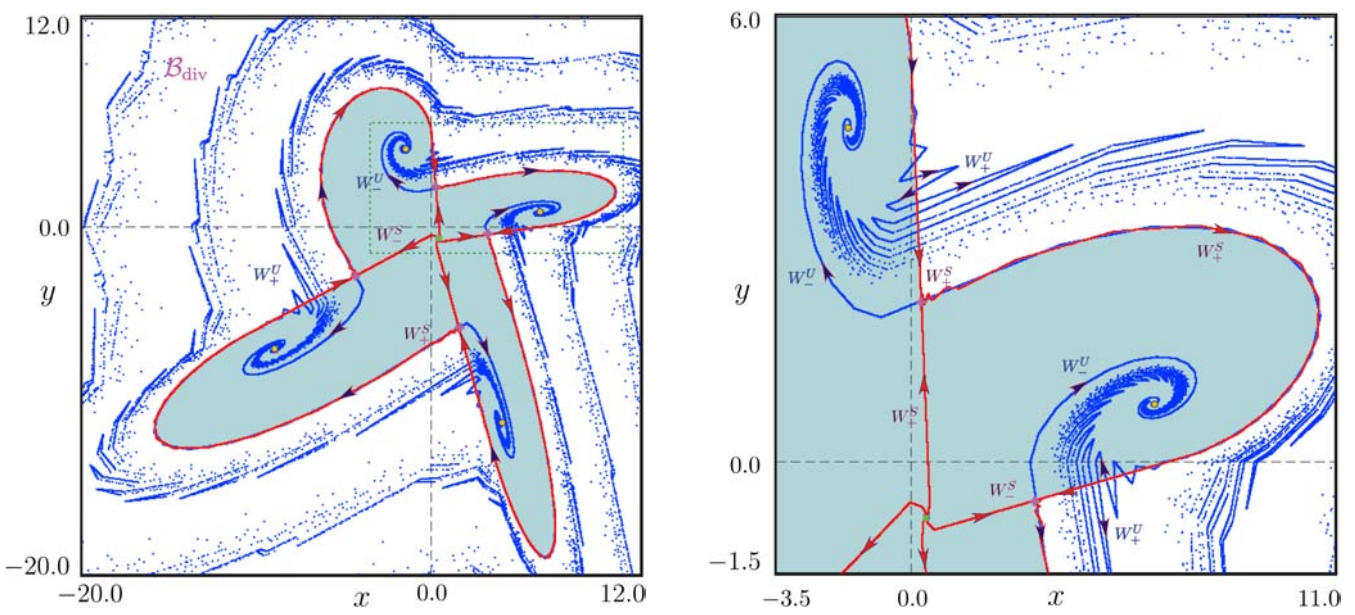

Fig. 15. Structure of the state space between the first and the second homoclinic bifurcations. The branches W^S_+ and W^U_+ of the stable and the unstable manifolds of the period-4 saddle cycle intersect transversely forming a homoclinic structure. Schematically this structure is shown in Fig. 18(c). The area marked by a rectangle in (a) is shown magnified in (b). Parameters: $\tau_{\mathcal{L}} = -0.5$, $\tau_{\mathcal{R}} = 0.34$, $\delta_{\mathcal{L}} = 0.5$, $\delta_{\mathcal{R}} = 1.8$, $\mu = 1$.

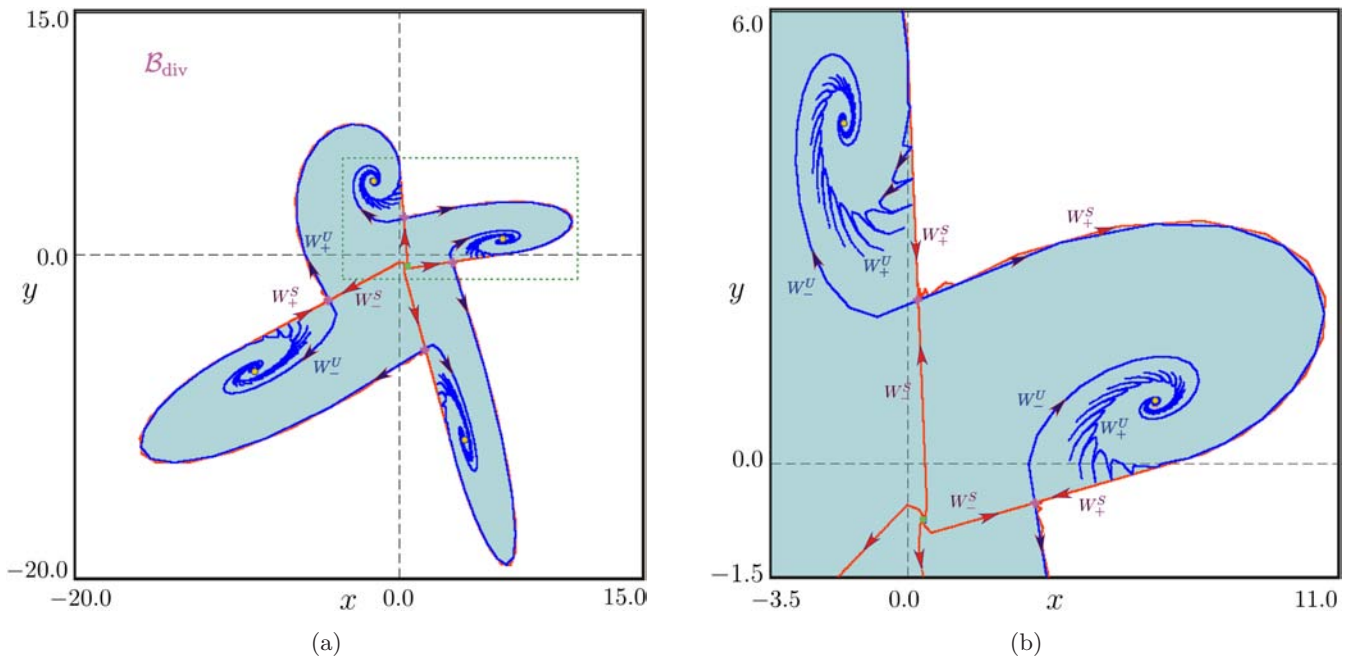

Fig. 16. Structure of the state space close to the second homoclinic bifurcation. At this bifurcation, the branches W_+^S of the stable manifold of the saddle cycle are touched "from inside" by the branches W_+^U of the unstable manifold (similarly to a homoclinic tangency in smooth maps). The area marked by a rectangle in (a) is shown magnified in (b). Parameters: $\tau_{\mathcal{L}} = -0.5$, $\tau_{\mathcal{R}} = 0.3405$, $\delta_{\mathcal{L}} = 0.5$, $\delta_{\mathcal{R}} = 1.8$, $\mu = 1$.

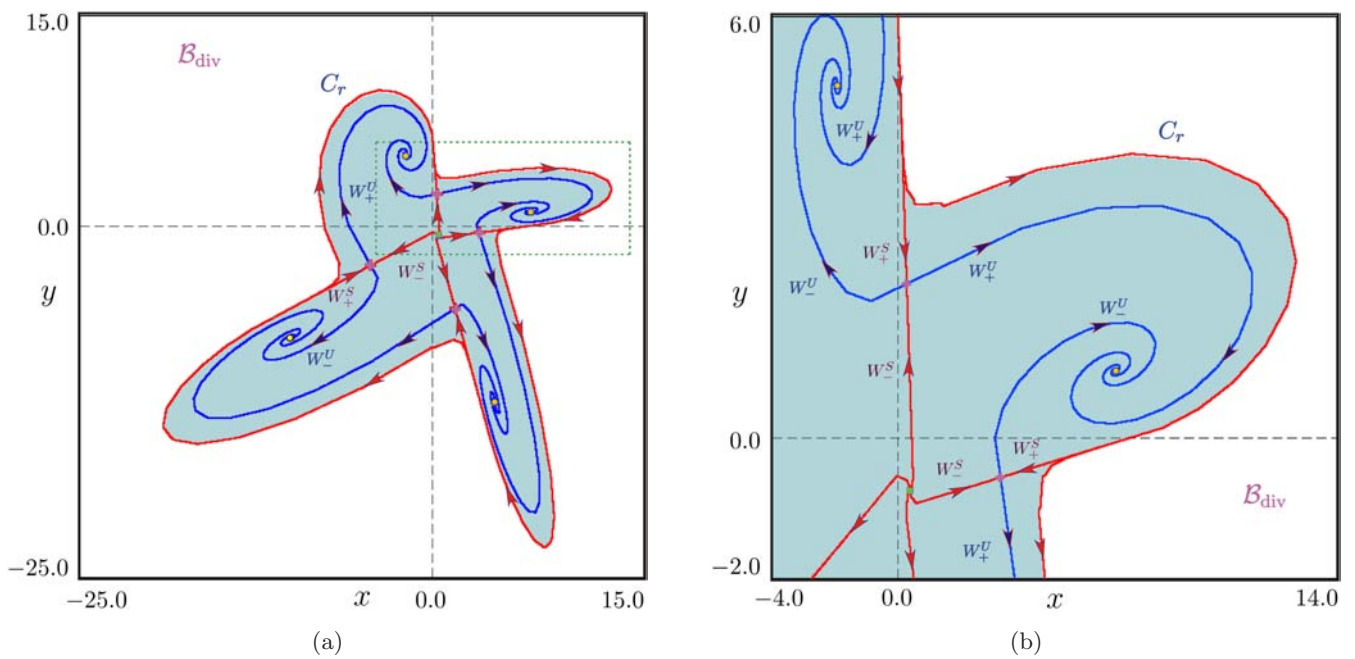

Fig. 17. Structure of the state space after the second homoclinic bifurcation at which a pair of closed invariant curves appear. The attracting closed invariant curve C_a includes two cycles, a saddle and a stable focus, and the saddle-focus connection composed of the unstable manifolds $W_\pm^U$ of the saddle cycle. The branches W_+^U of the saddle cycle come from the repelling closed curve C_r, which separates the basin of attraction of the stable motion from the divergent domain. The other branches W_-^U issue from the repelling focus fixed point. Schematically this structure is shown in Fig. 18(d). The area marked by a rectangle in (a) is shown magnified in (b). Parameters: $\tau_{\mathcal{L}} = -0.5$, $\tau_{\mathcal{R}} = 0.35$, $\delta_{\mathcal{L}} = 0.5$, $\delta_{\mathcal{R}} = 1.8$, $\mu = 1$.

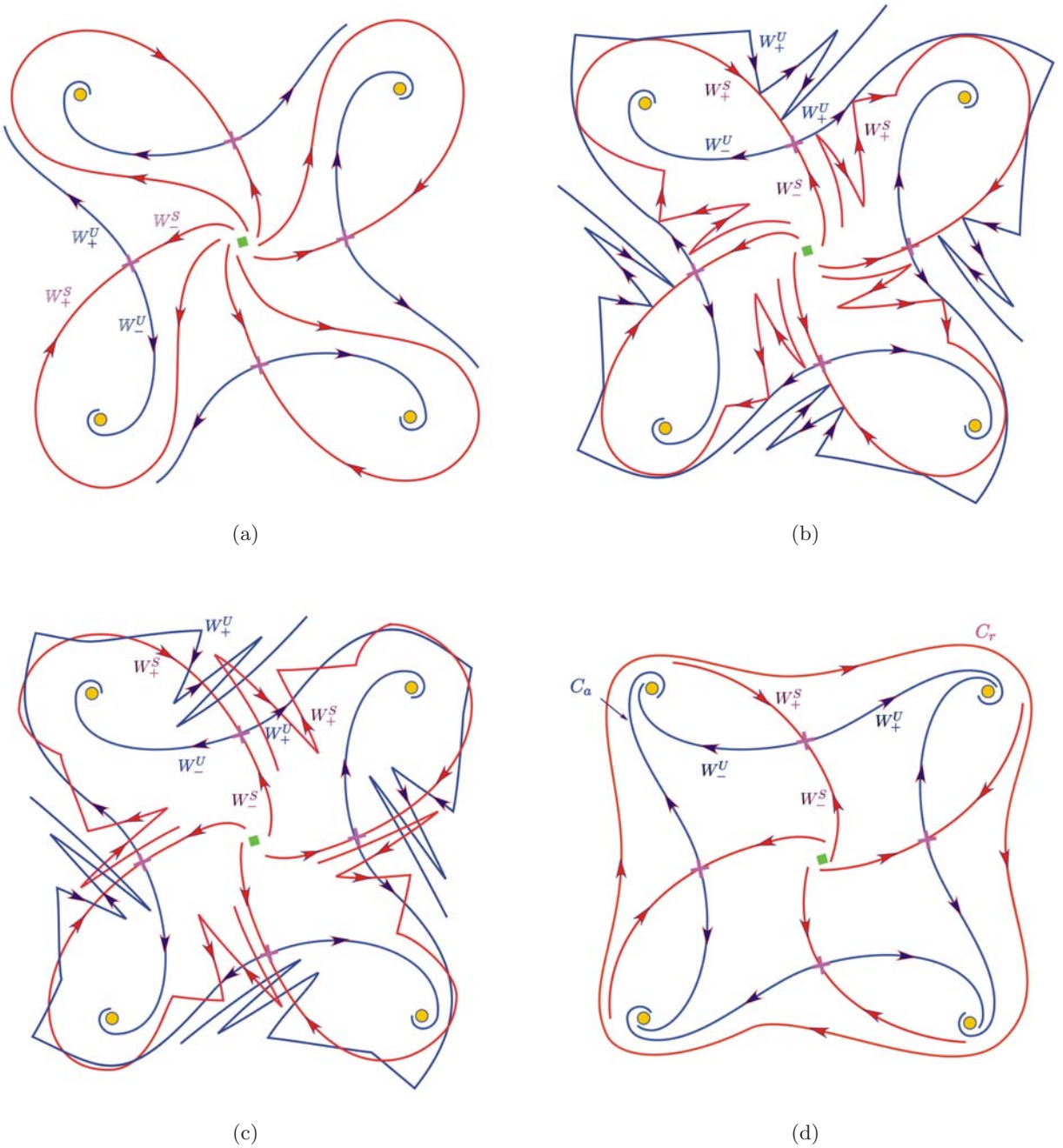

Fig. 18. Schematic representation of the structure of the state space (a) before the first homoclinic bifurcation (see Fig. 13); (b) at the first homoclinic bifurcation (see Fig. 14); (c) between the first and the second homoclinic bifurcations (see Fig. 15); (d) after the second homoclinic bifurcation (see Fig. 17).

contact the stable $W^S_\pm$ manifolds from the different side (see Fig. 16) than at the first homoclinic bifurcation. As a result of this bifurcation, a pair of closed invariant curves appear simultaneously, one attracting and one repelling, as illustrated in Figs. 17 and 18(d). The attracting set C_a includes two cycles, a saddle and a stable focus, and is formed by the saddle-focus connection composed of the unstable manifolds $W^U_\pm$ of the saddle cycle (Fig. 17). The stable manifolds of the saddle cycle come from different invariant repelling sets: the branches W^S_+ come from a repelling closed curve C_r, which separates the basin of attraction of the stable focus from the divergent domain $\mathcal{B}_{\rm div}$, and the other branches W^S_- issue from the repelling focus fixed point $\mathcal{O}_\mathcal{R}$.

6. Conclusion

Dangerous border collision bifurcations have been introduced as a special kind of border collision bifurcations in which the system under consideration has stable fixed points before and after the bifurcation, while the fixed point at the bifurcation moment is unstable as its basin of attraction shrinks to a set of measure zero. Later, this phenomenon has been understood from the theoretical point of view and has been observed experimentally. However, subsequent developments in the area of piecewise smooth systems have shown that the original definition of a dangerous border collision bifurcation is too restrictive as it excluded the possibility of attractors other than fixed points to be involved in a dangerous bifurcation.

In this paper we have proposed an extended definition which incorporates the possibility of having any kind of attractors before and after the bifurcation. Using the piecewise-linear normal form, we have explored some of the dynamical features that this extension offers. In particular, we found that there are two different types of dangerous border collision bifurcation in the sense of the extended definition.

The first mechanism was already known (as it applies for dangerous bifurcations in the sense of the original definition) and is typically (although not always) related to the existence of a singleton saddle cycle at the boundary between the basins of bounded and unbounded trajectories before and after the bifurcation. For this mechanism we have proved a general result that the same pair of cycles are associated with the event before and after the bifurcation, exchanging roles at the bifurcation point. That is why the regions of dangerous border collision bifurcation are symmetric in the parameter space with respect to the $\mu = 0$ subspace. We have also summarized the calculation procedure for these regions. We have discovered a second type of dangerous bifurcations in the sense of the extended definition, in which the boundary between convergent and divergent domains in the phase space is formed by a repelling closed invariant curve. This invariant curve may be associated either with phase-locked or with quasiperiodic dynamics. In the presented example of the latter case we have shown how this invariant curve appears together with an attracting one, which is formed by a saddle-focus connection. Both invariant curves appear simultaneously as a result of a sequence of two homoclinic bifurcations which are similar to homoclinic tangencies in smooth maps.

Acknowledgments

The work of V. Avrutin was partially supported by the German Research Foundation within the scope of the project "Organizing centers in discontinuous dynamical systems: bifurcations of higher codimension in theory and applications". The work of L. Gardini has been done within the activities of the GNFM (National Group of Mathematical Physics, INDAM Italian Research Group).

References

Armstrong-Hélouvry, B., Dupont, P. & Wit, C. D. [1994] "A survey of models, analysis tools and compensation methods for the control of machines with friction," *Automatica* **30**, 1083–1138.

Avrutin, V., Gardini, L. & Schanz, M. [2010] "On a special type of border-collision bifurcations occurring at infinity," *Physica D* **239**, 1083–1094.

Avrutin, V., Schanz, M. & Banerjee, S. [2012] "Occurrence of multiple attractor bifurcations in the two-dimensional piecewise linear normal form map," *Nonlin. Dyn.* **67**, 293–307.

Banerjee, S., Yorke, J. A. & Grebogi, C. [1998] "Robust chaos," *Phys. Rev. Lett.* **80**, 3049.

Banerjee, S. & Grebogi, C. [1999] "Border collision bifurcations in two-dimensional piecewise smooth maps," *Phys. Rev. E* **59**, 4052.

Banerjee, S., Ranjan, P. & Grebogi, C. [2000] "Bifurcations in two-dimensional piecewise smooth maps — theory and applications in switching circuits," *IEEE Trans. Circuits Syst.-I*: *Fund. Th. Appl.* **47**, 633–643.

Banerjee, S. & Verghese, G. C. [2001] *Nonlinear Phenomena in Power Electronics — Attractors, Bifurcations, Chaos, and Nonlinear Control* (IEEE Press).

Bischi, G. I. & Merlone, U. [2010] *Global Dynamics in Adaptive Models of Collective Choice with Social Influence* (Birkhäuser, Boston), pp. 223–244.

Brogliato, B. [1999] *Nonsmooth Mechanics*, Communications and Control Engineering (Springer).

Deane, J. H. & Hamill, D. C. [1990] "Instability, subharmonics, and chaos in power electronic systems," *IEEE Trans. Power Electron.* **5**, 260–268.

Di Bernardo, M., Feigin, M., Hogan, S. & Homer, M. [1999] "Local analysis of c-bifurcations in n-dimensional piecewise-smooth dynamical systems," *Chaos Solit. Fract.* **10**, 1881–1908.

Do, Y. & Baek, H. K. [2006] "Dangerous border-collision bifurcations of a piecewise-smooth map," *Commun. Pure Appl. Anal.* **5**, 493.

Do, Y. [2007] "A mechanism for dangerous border collision bifurcations," *Chaos Solit. Fract.* **32**, 352–362.

Dutta, M., Nusse, H. E., Ott, E., Yorke, J. A. & Yuan, G. [1999] "Multiple attractor bifurcations: A source of unpredictability in piecewise smooth systems," *Phys. Rev. Lett.* **83**, 4281.

Foroni, I. & Agliari, A. [2011] "Complex dynamics associated with the appearance/disappearance of invariant closed curves," *Math. Comput. Simul.* **81**, 1640–1655.

Ganguli, A. & Banerjee, S. [2005] "Dangerous bifurcation at border collision: When does it occur?" *Phys. Rev. E* **71**, 057202-1–057202-4.

Gardini, L., Avrutin, V. & Schanz, M. [2009] "Connection between bifurcations on the Poincaré equator and dangerous bifurcations," *Iteration Theory*, eds. Sharkovsky, A. & Sushko, I. (Grazer Math. Ber.), pp. 53–72.

Hassouneh, M. A., Abed, E. H. & Nusse, H. E. [2004] "Robust dangerous border-collision bifurcations in piecewise smooth systems," *Phys. Rev. Lett.* **92**, 070201.

Kousaka, T., Ueta, T. & Kawakami, H. [1999] "Bifurcation of switched nonlinear dynamical systems," *IEEE Trans. Circuits Syst.-II*: *Anal. Dig. Sign. Process.* **46**, 878–885.

Kuznetsov, Y. [2004] *Elements of Applied Bifurcation Theory*, 3rd edition (Springer).

Leine, R. & Nijmeijer, H. [2013] *Dynamics and Bifurcations of Non-Smooth Mechanical Systems*, Vol. 18 (Springer Science & Business Media).

Leonov, N. [1959] "Map of the line onto itself," *Radiofisica* **3**, 942–956.

Leonov, N. [1962] "Discontinuous point transformation of a straight line into a straight line," *Dokl. Akad. Nauk SSSR* **143**, 1038.

Matsuyama, K., Sushko, I. & Gardini, L. [2016] "Revisiting the model of credit cycles with good and bad projects," *J. Econ. Th.* **163**, 525–556.

Nordmark, A. B. [1991] "Non-periodic motion caused by grazing incidence in an impact oscillator," *J. Sound Vibr.* **145**, 279–297.

Nusse, H. E. & Yorke, J. A. [1992] "Border-collision bifurcations including 'period two to period three' bifurcation for piecewise smooth systems," *Physica D* **57**, 39–57.

Nusse, H. E. & Yorke, J. A. [1995] "Border-collision bifurcations for piecewise smooth one dimensional maps," *Int. J. Bifurcation and Chaos* **5**, 189–207.

Puu, T. & Sushko, I. (eds.) [2002] *Oligopoly Dynamics — Models and Tools* (Springer-Verlag).

Puu, T. & Sushko, I. (eds.) [2006] *Business Cycle Dynamics — Models and Tools* (Springer-Verlag).

Saha, A. & Banerjee, S. [2016] "Existence and stability of periodic orbits in n-dimensional piecewise linear continuous maps," http://arXiv.org/pdf/1504.01899v2.pdf.

Simpson, D. [2014] "Sequences of periodic solutions and infinitely many coexisting attractors in the border-collision normal form," *Int. J. Bifurcation and Chaos* **24**, 1430018.

Sushko, I. & Gardini, L. [2008] "Center bifurcation for a two-dimensional border-collision normal form," *Int. J. Bifurcation and Chaos* **18**, 1029–1050.

Sushko, I. & Gardini, L. [2010] "Degenerate bifurcations and border collisions in piecewise smooth 1D and 2D maps," *Int. J. Bifurcation and Chaos* **20**, 2045–2070.

Zhusubaliyev, Zh. T. & Mosekilde, E. [2003] *Bifurcations and Chaos in Piecewise-Smooth Dynamical Systems*, Nonlinear Science Series A, Vol. 44 (World Scientific).

Zhusubaliyev, Zh. T., Mosekilde, E., Maity, S., Mohanan, S. & Banerjee, S. [2006] "Border-collision route to quasiperiodicity: Numerical investigation and experimental confirmation," *Chaos* **16**, 023122.

Zhusubaliyev, Zh. T. & Mosekilde, E. [2015] "Multistability and hidden attractors in a multilevel dc/dc converter," *Math. Comput. Simul.* **109**, 32–45.

Appendix A
Proof of Eqs. (10) and (15)

Instead of proving particular Eqs. (10) and (15) we can prove the following more general statement, describing the equivalence of regions related to dangerous bifurcations for $\mu > 0$ and $\mu < 0$:

Proposition 1. *Suppose that for* $\mu > 0$

(i) *There exist two cycles* $\mathcal{O}_\sigma$ *and* $\mathcal{O}_\varrho$ *and with the existence regions satisfying* $\mathcal{P}_\varrho^{(+)} \subsetneq \mathcal{P}_\sigma^{(+)}$.

(ii) *The region* $\mathcal{D}_\sigma^{(+)} \subset \mathcal{P}_\sigma^{(+)} \backslash \mathcal{P}_\varrho^{(+)}$ *is confined by two boundaries* η_σ *and* η_ϱ *associated with codimension-1 degenerate transcritical bifurcations of the cycles* $\mathcal{O}_\sigma$ *and* $\mathcal{O}_\varrho$, *respectively.*

(iii) *The region* $\mathcal{D}_\sigma^{(+)}$ *is not intersected by any curves* $N_j = 0$ *or* $D = 0$ *where* N_j *and* D *are as given by Eq. (A.3) for* $\mathcal{O}_\sigma$ *and* $\mathcal{O}_\varrho$.

Then for $\mu < 0$

- *the cycles* $\mathcal{O}_\sigma$ *and* $\mathcal{O}_\varrho$ *exist*;
- *the existence regions of the cycles* $\mathcal{P}_\sigma^{(-)}$ *and* $\mathcal{P}_\varrho^{(-)}$ *(neglecting the sign of* μ*) differ from* $\mathcal{P}_\sigma^{(+)}$ *and* $\mathcal{P}_\varrho^{(+)}$;

- *however, there is a region* $\mathcal{D}_{\varrho}^{(-)} \subset \mathcal{P}_{\varrho}^{(-)} \backslash \mathcal{P}_{\sigma}^{(-)}$ *which is confined by the same two boundaries* η_σ *and* η_ϱ *as for* $\mu > 0$ *and therefore coincides with* $\mathcal{D}_{\sigma}^{(-)}$ *(neglecting the sign of* μ*).*

To prove this proposition, we use the following notation. Let

$$\mathcal{O}_\sigma = \{X_j = (x_j, y_j)^{\mathrm{T}}\}_{j=0}^{m-1} \tag{A.1}$$

be an m-cycle of map (1) corresponding to the symbolic sequence

$$\sigma = \sigma_0 \sigma_1 \cdots \sigma_{m-1} \tag{A.2}$$

with $\sigma_j \in \{\mathcal{L}, \mathcal{R}\}$.

Remark 1. It can be shown that the analytic expressions of the x-components of the points of $\mathcal{O}_\sigma$ can be written as

$$x_0 = \frac{\mu N_0}{D}, x_1 = \frac{\mu N_1}{D}, \ldots, x_{m-1} = \frac{\mu N_{m-1}}{D} \tag{A.3}$$

with the following properties:

(i) All expressions for x_j, $j = 0, \ldots, m-1$ have the same denominator D.
(ii) All expressions for N_j, $j = 0, \ldots, m-1$ and D do not depend on μ but on $\tau_\mathcal{L}$, $\tau_\mathcal{R}$, $\delta_\mathcal{L}$, $\delta_\mathcal{R}$ only.
(iii) All expressions for x_j, $j = 0, \ldots, m-1$ have the same linear factor μ.

Remark 2. Recall that the cycle $\mathcal{O}_\sigma$ exists if the points X_j are located in the left/right half-planes in accordance with the symbolic sequence σ. More precisely, the cycle exists iff each of the conditions from the following set

$$\mathcal{C} = \{c_j\}_{j=0}^{m-1} \quad \text{with } c_j = \begin{cases} x_j \le 0 & \text{if } \sigma_j = \mathcal{L} \\ x_j \ge 0 & \text{if } \sigma_j = \mathcal{R} \end{cases} \tag{A.4}$$

is satisfied. Otherwise the cycle does not exist and is called virtual.

Now let us introduce the *virtuality index* $\varkappa$ of a cycle $\mathcal{O}_\sigma$ defined at a point $\tau_{\mathcal{L}/\mathcal{R}}$, $\delta_{\mathcal{L}/\mathcal{R}}$, μ in the parameter space as *the number of the conditions from the set* $\mathcal{C}$ *which are violated* at this point:

$$\varkappa : \{\sigma, \tau_{\mathcal{L}/\mathcal{R}}, \delta_{\mathcal{L}/\mathcal{R}}, \mu\} \to \{0, \ldots, m\}. \tag{A.5}$$

Clearly, *the cycle exists iff* $\varkappa$ *is zero.*

The key point of the proof of Proposition 1 is to show how the virtuality index $\varkappa$ changes if the parameters are varied across several bifurcations boundaries. For the proof below we need the following two properties:

Property 1. *If* μ *is kept fixed and* $\tau_{\mathcal{L}/\mathcal{R}}, \delta_{\mathcal{L}/\mathcal{R}}$ *are varied across a codimension-1 degenerate transcritical bifurcation boundary from inside the existence region of a cycle to outside, then for this cycle the index* $\varkappa$ *changes from zero to* m*.*

Proof. Recall that a degenerate transcritical bifurcation corresponds to the condition $D = 0$ in Eq. (A.3). If the parameters are varied across such a boundary, then each value x_j, $j = 0, \ldots, m-1$, changes its sign. Accordingly, as before the bifurcation all m conditions (A.4) from the set $\mathcal{C}$ are satisfied ($\varkappa = 0$), so after the bifurcation all of them are violated ($\varkappa = m$). ■

Property 2. *If* $\tau_{\mathcal{L}/\mathcal{R}}, \delta_{\mathcal{L}/\mathcal{R}}$ *are kept fixed and for* $\mu > 0$ *the virtuality index of a cycle is* $\varkappa = k$ *with* $0 \le k \le m$*, then for* $\mu < 0$ *the virtuality index of this cycle is* $\varkappa = m - k$*.*

Proof. Since N_j, $j = 0, \ldots, m-1$, and D depend on $\tau_{\mathcal{L}/\mathcal{R}}$, $\delta_{\mathcal{L}/\mathcal{R}}$ only, and these parameters are kept fixed, the effect of μ varied through zero is that each value x_j, $j = 0, \ldots, m-1$, changes its sign. Accordingly, each condition in (A.4) which is satisfied for $\mu > 0$ becomes violated, and each violated condition becomes satisfied. This corresponds to a transition from $\varkappa = k$ to $\varkappa = m - k$. ■

Now we can provide the following.

Proof of Proposition 1. The idea of the proof is simple: when starting in the existence region of a cycle ($\varkappa = 0$) and changing the parameters across the boundary given by a degenerate transcritical bifurcation curve, we obtain for this cycle $\varkappa = m$. Eventually changing the sign of μ we recover $\varkappa = 0$, so that the cycle necessarily exists again.

More precisely, let us consider first the case $\mu > 0$. In the schematic picture shown in Fig. 19(a) the region $D_\sigma^{(+)}$ is confined by the curves η_σ and η_ϱ associated with degenerate transcritical bifurcations of the cycles $\mathcal{O}_\sigma$ and $\mathcal{O}_\varrho$, respectively. Let $P_1^{(+)}$ be the region in the parameter space separated from $D^{(+)}$ by η_ϱ [on the right side of $D^{(+)}$ in Fig. 19(a)] and $P_2^{(+)}$ the region separated from $D^{(+)}$ by η_σ [on the left side of $D^{(+)}$ in Fig. 19(a)]. Let $A_1^{(+)}$ be a point in the region $P_1^{(+)}$ sufficiently close to η_ϱ and $B_1^{(+)}$ be a point in the region $D^{(+)}$ sufficiently close to $A^{(+)}$.

As at η_ϱ the cycle $\mathcal{O}_\varrho$ undergoes a degenerate transcritical bifurcation, it is guaranteed that

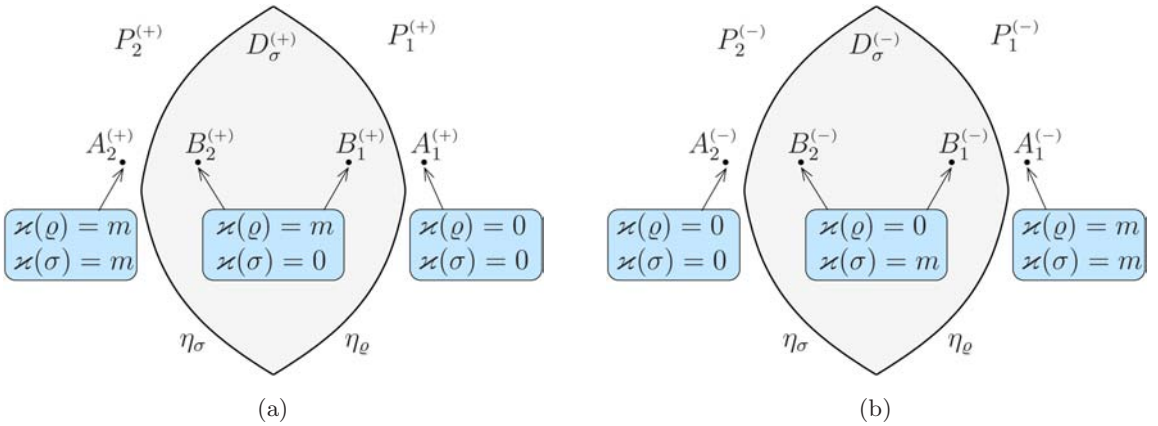

Fig. 19. Schematic representation of the regions in the $(\tau_\mathcal{L}, \tau_\mathcal{R}, \delta_\mathcal{L}, \delta_\mathcal{R})$ parameter space in which the cycles $\mathcal{O}_\sigma$ and $\mathcal{O}_\varrho$ exist for (a) $\mu > 0$ and (b) $\mu < 0$.

before the bifurcation the cycle exists, and hence also $\mathcal{O}_\sigma$ (by assumption (i)), i.e. $\varkappa(\sigma, A_1^{(+)}) = 0$ and $\varkappa(\varrho, A_1^{(+)}) = 0$. Then, after the parameters are varied across η_ϱ the virtuality index becomes $\varkappa(\varrho, B_1^{(+)}) = m$ by Property 1, while $\varkappa(\sigma, B_1^{(+)}) = 0$ remains. By assumption (iii) these values are valid in the complete region $\mathcal{D}_\sigma^{(+)}$ and in particular at a point $B_2^{(+)}$ located inside $D_\sigma^{(+)}$ close to the boundary η_σ. Then at a point $A_2^{(+)}$ located sufficiently close to $B_2^{(+)}$ but outside $D_\sigma^{(+)}$ we obtain $\varkappa(\sigma, A_2^{(+)}) = m$ (by Property 1), while $\varkappa(\varrho, A_2^{(+)}) = m$ remains.

Next let us change the sign of μ. As D does not depend on μ, the curves η_σ and η_ϱ do remain the same. Property 2 implies that in the region between these curves it holds $\varkappa(\sigma, B_{1,2}^{(-)}) = m$ and $\varkappa(\varrho, B_{1,2}^{(-)}) = 0$, i.e. cycle $\mathcal{O}_\varrho$ exists in the region between these curves (denoted accordingly by $D_\varrho^{(-)}$) while the cycle $\mathcal{O}_\sigma$ does not. Similarly, $\varkappa(\sigma, A_2^{(-)}) = 0$ and $\varkappa(\varrho, A_2^{(-)}) = 0$, i.e. both cycles exist in the region $\mathcal{P}_2^{(-)}$, and $\varkappa(\sigma, A_2^{(-)}) = m$, $\varkappa(\varrho, A_2^{(-)}) = m$, i.e. no one cycle exists in the region $\mathcal{P}_1^{(-)}$. ■

Clearly, Eqs. (10) and (15) follow from the Proposition 1 with $\sigma = \mathcal{R}\mathcal{L}^{k-1}\mathcal{R}$, $\varrho = \mathcal{R}\mathcal{L}^k$ and $\sigma = \mathcal{L}\mathcal{R}^k$, $\varrho = \mathcal{L}\mathcal{R}^{k-1}\mathcal{L}$, respectively.

Remark 3. The described structure can be summarized as follows. For $\mu > 0$ in the region $\mathcal{P}_1^{(+)}$ both cycles $\mathcal{O}_\sigma$ and $\mathcal{O}_\varrho$ exist. When the parameters are varied across the boundary η_ϱ the cycle $\mathcal{O}_\varrho$ disappears in a degenerate transcritical bifurcation. After this boundary the cycle does not exist for $\mu > 0$ but necessarily appears for $\mu < 0$. Note also that the degenerate transcritical bifurcation corresponds to the condition that one of the eigenvalues of the cycle is $+1$, and the expressions for the eigenvalues do not depend on μ. Hence, the stability of the cycle changes at η_ϱ in the following way:

(a) if the cycle $\mathcal{O}_\varrho$ disappears at η_ϱ for $\mu > 0$ stable, then it appears at η_ϱ for $\mu < 0$ unstable, and vice versa;
(b) the same applies to the cycle $\mathcal{O}_\sigma$ which exists for $\mu > 0$ in the regions $\mathcal{P}_1^{(+)}$ and $D_\sigma^{(+)}$, disappears at η_σ, and appears at this curve again for $\mu < 0$, changing its stability.

Appendix B
Calculation of the Parameter Regions of Dangerous Bifurcations

The calculation of the parameter regions in which a variation of μ across zero leads to a dangerous bifurcation differs depending on the type of the bifurcation. For the novel type reported in this paper and leading to the bounded basin boundary (see Sec. 5.2), the possible calculation procedures are closely related to the detection of pair of cycles saddle-repelling node or saddle-repelling focus and to the existence of related homoclinic connections or homoclinic tangles. These procedures are not yet well developed. By contrast, for the previously known mechanism leading to the basin boundary of $\mathcal{B}_{\text{div}}$ that extends to infinity (see Sec. 5.1), the calculation procedure is as follows:

(1) determine the pair of complementary cycles related to the particular region of dangerous bifurcations;

(2) determine the bifurcation boundaries associated with degenerate transcritical bifurcations of these cycles.

Note that for the calculation of the degenerate transcritical bifurcation curves one can use the condition that one of the eigenvalues of the corresponding cycle becomes +1. However, it is easier to use the condition that the denominator in the expression of any point of the cycle becomes zero. In [Ganguli & Banerjee, 2005] it is shown that the later condition implies the former one.

Clearly, the applicability of the described procedure for analytic calculation of the boundaries of regions associated with dangerous bifurcations is restricted by the complexity of the involved expressions which grows with increasing periods of the corresponding cycles. Therefore, in previous publications the described procedure has been applied for cycles with relatively low periods. However, the results reported recently in [Saha & Banerjee, 2016] make it possible to extend the applicability of the calculation procedure. To illustrate the idea of this extension let us consider as an example the calculation of the boundaries of the regions of dangerous bifurcations reported in the original publications [Ganguli & Banerjee, 2005]. These boundaries are given by the degenerate transcritical bifurcation curves $\eta_{\mathcal{LR}^k}$ and $\eta_{\mathcal{LR}^{k-1}\mathcal{L}}$ of the cycles $\mathcal{O}_{\mathcal{LR}^k}$ and $\mathcal{O}_{\mathcal{LR}^{k-1}\mathcal{L}}$, respectively. To obtain the analytic expression for these curves we can compute any one point for each of the associated cycles. Then, equating the denominators in these expressions to zero, we obtain parameter values at which the points of the cycle approach infinity, and the cycle appears/disappears via a degenerate transcritical bifurcation. By extension of Leonov's method [Leonov, 1959, 1962] as used in [Avrutin *et al.*, 2012], it can be shown that for the map (1) a point on the cycle $\mathcal{O}_{\mathcal{RL}^k}$ is given by

$$(I - A_{\mathcal{L}}^k A_{\mathcal{R}})^{-1}(A_{\mathcal{L}}^k + \phi_{\mathcal{L},k})B, \tag{B.1}$$

where

$$\phi_{\mathcal{L},k} = (I - A_{\mathcal{L}})^{-1}(I - A_{\mathcal{L}}^k). \tag{B.2}$$

Similarly, a point of the cycle $\mathcal{O}_{\mathcal{RL}^{k-1}\mathcal{R}}$ is given by

$$(I - A_{\mathcal{L}}^{k-1}A_{\mathcal{R}}^2)^{-1}(A_{\mathcal{L}}^k(I + A_{\mathcal{R}}) + \phi_{\mathcal{L},k})B. \tag{B.3}$$

As one can see, expressions in Eqs. (B.1) and (B.3) force us to calculate high powers of the matrix $A_{\mathcal{L}}$. Similar calculations for other cycles may require to calculate high powers of the matrix $A_{\mathcal{R}}$ as well. This can easily be done due to the following

Proposition 2. *For all $k \geq 1$ the kth power of the matrix*

$$A = \begin{pmatrix} \tau & 1 \\ -\delta & 0 \end{pmatrix} \tag{B.4}$$

is given by

$$A^k = \begin{pmatrix} a_k & a_{k-1} \\ -\delta a_{k-1} & -\delta a_{k-2} \end{pmatrix} \tag{B.5}$$

where

$$\begin{aligned} &a_k = \tau a_{k-1} - \delta a_{k-2}, \\ &a_0 = 1, \quad a_{-1} = 0. \end{aligned} \tag{B.6}$$

This result has been mentioned in [Sushko & Gardini, 2008]. A proof which applies not only in $\mathbb{R}^2$ but also in the general case $\mathbb{R}^n$, $n \geq 2$ can be found in [Saha & Banerjee, 2016]. Note also that Eq. (B.6) has an explicit solution so that the necessary powers of the matrices $A_{\mathcal{L}}$ and $A_{\mathcal{R}}$ can be calculated immediately, without iterating Eq. (B.6):

$$a_k = \frac{1}{\Delta}\left(\left(\frac{2\delta}{\tau - \Delta}\right)^{k+1} - \left(\frac{2\delta}{\tau + \Delta}\right)^{k+1}\right) \quad \text{if } \tau^2 - 4\delta > 0 \tag{B.7}$$

$$a_k = (1 + k)\left(\frac{\tau}{2}\right)^k \quad \text{if } \tau^2 - 4\delta = 0 \tag{B.8}$$

$$a_k = \sqrt{\delta^k}\left(\cos(\theta k) + \frac{\tau}{\sqrt{4\delta - \tau^2}}\sin(\theta k)\right) \quad \text{if } \tau^2 - 4\delta < 0 \tag{B.9}$$

where

$$\Delta = \sqrt{\tau^2 - 4\delta}, \quad \cos(\theta) = \frac{\tau}{2\delta},$$

$$\sin(\theta) = \frac{\sqrt{4\delta - \tau^2}}{2\delta}.$$